

Uncertainty in deriving dispersion parameters from meteorological data

A report prepared for ADMLC by

V Auld, R Hill, T J Taylor

Westlakes Scientific Consulting

This study was funded by the UK Atmospheric Dispersion Modelling Liaison Committee.

The views expressed in this report are those of the authors, and do not necessarily represent the views of ADMLC or of any of the organisations represented on it

EXECUTIVE SUMMARY

Atmospheric dispersion models are frequently used for assessing the dispersion of pollutants in order to determine concentrations at local sensitive receptors. The models are used by both emergency planners, to determine under what conditions to implement accident plans, and by environmental assessors and regulators, to quantify the impact of proposed or current emissions. The uncertainty associated with deterministic model predictions of long and short term concentrations is an issue of concern to all users. This study was funded by ADMLC, the Atmospheric Dispersion Modelling Liaison Committee, to investigate the uncertainty in model predictions due to meteorological data input and the subsequent treatment of that input within Gaussian models.

The report briefly reviews the measurement techniques and instrument accuracies associated with meteorological data most frequently used by the modelling community. It discusses issues of representativity of the measured and estimated boundary layer parameters input by the model user, such as roughness length, albedo and Bowen ratio. The treatment of the meteorological data within ADMS and AERMOD is discussed in detail, the relevant differences between the model's meteorological pre-processors are identified and their influences on boundary layer structure and plume dispersion calculations are considered.

The use of alternative meteorological data sources, such as flux profile measurements, sonic anemometers and the use of NWP (numerical weather prediction) data are evaluated. The review aimed to establish whether there are viable alternatives to the current dependence upon the model pre-processors to estimate boundary layer stability parameters. In the absence of representative site measurements, the use of NWP data is recommended after encouraging comparisons with site data. Potential improvements to the current NWP dataset provided by the Met Office are suggested and further feasibility studies recommended. Specific conditions where meteorological input to ADMS and AERMOD result in disparate predictions are identified and investigated, and the results of a probabilistic assessment of uncertainty associated with meteorological input to ADMS are discussed.

This study illustrates that the accuracy of meteorological systems measuring standard parameters such as wind speed, direction and temperature contribute little towards the overall uncertainty of the model predictions. The main factors considered when discussing the 'representativity' of meteorological data include distance between the measurement site and industrial site, the matching of surface characteristics at each site (particularly roughness length), and the local terrain (including coastal influences). Results from several sections of the report identify roughness length as a parameter whose contribution to overall model uncertainty was significant. A concerted attempt to provide the model with realistic input of this parameter for both the meteorological site and within the chosen model domain should reduce the uncertainty associated with predictions.

Peak concentrations often occur during periods of low wind speeds, and agreement between models under these conditions is poor. Poor agreement is also found during dusk periods and periods where there is rapid change in cloud cover. If the model user is particularly concerned with modelling these conditions, or where results are close to benchmark concentrations, they are recommended to consider obtaining predictions from more than one model. The results of the study concentrate on a 40 m stack release scenario and further investigation of meteorological uncertainty for releases at different stack heights is proposed. Throughout the report, the authors have intended to highlight findings of relevance to the model users, with the main guidance summarised in the final section.

CONTENTS

1	Introduction	1
2	Measurement methods and accuracy of meteorological parameters	2
2.1	Ringway 2000 meteorological data	4
2.2	Wind field	4
2.3	Temperature and relative humidity	5
2.4	Precipitation	5
2.5	Cloud cover	6
2.6	Solar radiation	6
3	Representativity of meteorological parameters	7
3.1	Low wind speeds and calm conditions	9
3.2	Data gaps	10
3.3	Atmospheric stability	10
3.4	Surface energy balance parameters	11
3.5	Surface roughness	12
4	Treatment of meteorological input within ADMS and AERMOD	13
4.1	Meteorology	13
4.2	Meteorological pre-processors	14
4.3	Boundary layer structure calculations	17
4.4	Plume dispersion	17
4.4.1	Dispersion parameter estimation	19
4.5	Summary	22
5	Evaluation of alternative methods for estimating boundary layer parameters for dispersion models	23
5.1	Eddy-correlation method	24
5.2	Flux-gradient method	24
5.2.1	Assessment of the errors in applying flux gradient methods	25
5.3	Numerical weather prediction datasets	28
5.3.1	Comparison of NWP data and coastal site measurements and their impact on ADMS predictions	29
5.4	Summary	30
6	ADMS and AERMOD disparities due to treatment of meteorological inputs	31
6.1	Methods	31
6.2	Results	33
6.2.1	Correlation between yearly distributions of boundary layer parameters	33
6.2.2	Comparison of annual average model concentration predictions	35
6.2.3	Comparison of peak short term model concentration predictions	36
6.2.4	Comparison of model predictions from representative days	37
6.3	Summary	37
7	Probabilistic modelling of uncertainty due to meteorological input to ADMS	38

7.1	Methods	38
7.2	Determining appropriate probability distributions	40
7.2.1	Uncertainty in basic meteorology	40
7.2.2	Uncertainty in the surface energy budget	41
7.2.3	Uncertainty in the roughness length	42
7.3	Results	42
7.4	Summary	44
8	Guidance for the model user community	45
9	Recommendations for further investigation	47
10	References	48
11	Symbols and notation	51
12	Tables	55
13	Figures	66
APPENDIX A Reconstructing temperature and wind speed profiles		73
A1	Interpreting profiles to estimate boundary layer parameters	73
A2	Interpreting boundary layer parameters to estimate profiles	74

1 INTRODUCTION

Dispersion modelling tools are used to support emergency response decision making in the event of accidental or otherwise unscheduled discharges. They are also used to assess the environmental impacts of atmospheric releases with regard to the granting of planning permission and authorisation of site operation licenses. Whether using a simple robust and efficient R91 (Clark, 1979) based Gaussian model, or a more advanced commercial Gaussian-like model such as ADMS (Carruthers et al, 1994; CERC, 2001) or AERMOD (Cimorelli et al, 2002), all model users are required to consider the uncertainty attached to the model's deterministic predictions. There continues to be a dissociation between the models estimated ranges of certainty and the increasing accuracy of prediction required to fulfil the needs of the decision makers and regulators.

Regulators are often required to make planning and discharge authorisation decisions on the basis of model predictions alone, in the absence of detailed site specific measurements. The impact of emissions is routinely assessed against air quality standards based on either the annual average concentration of a pollutant or on a certain percentile of the annual distribution of air concentrations, averaged over a particular time period. For example, nitrogen dioxide air concentrations are regulated as both annual average ($40 \mu\text{g m}^{-3}$) and the 99.8th percentile of the hourly concentration distribution for a given year. An alternative way of interpreting the 99.8th percentile of hourly averaged air concentrations is the 18th highest hourly air concentration value over the full period of a year.

Emergency decision makers rely on a dispersion modelling assessment to provide a rapid, robust and potentially conservative (maximum) estimate of short term concentrations downwind of an emission source. All model users would benefit from knowledge of the likely range of uncertainty associated with the single value provided for their purpose, and also from an understanding of which parameters are the dominant contributors towards this ambiguity.

This study concentrates on the uncertainties associated with the user's choice and model's treatment of meteorological data. It is recognised that further ambiguities are associated with confidence in the inputs of emission rates, stack characteristics, the model's treatment of terrain and buildings, and the user's choice of input parameters and output format. Beyond the dispersion modelling of pollutants are additional uncertainties such as obtaining a true 'background' concentration against which to analyse the contribution of a site's proposed emissions. Perhaps the largest uncertainty of all within an environmental assessment is that associated with the final outcome, ie, the level of exposure and relative risk that each pollutant of concern might pose to the health of members of the public.

Both the AERMOD system and ADMS contain meteorological pre-processors that are used to derive boundary layer parameters from commonly measured

meteorological data. For the UK, the primary data used as input to these models are surface wind speeds, wind direction, temperature and cloud cover estimates. AERMOD and ADMS use similar basic meteorological and dispersion assumptions, yet comparisons of their predictions for matched input data can occasionally be significantly different. Hall et al (2000) concluded in their model inter-comparison study that the large differences they observed in predicted concentrations might be due to the different treatment of meteorological data within the met pre-processors. Within this study we have aimed to identify, describe and understand such possible disparities between the models.

The report briefly reviews the measurement techniques and instrument accuracies associated with meteorological data most frequently used by the modelling community. This is followed by a discussion on the representativity of the measured parameters and that of the boundary layer and surface parameters which are input directly and/or estimated within the model pre-processors.

The model's treatment of the meteorological data is discussed in detail, identifying relevant differences between the pre-processors and their influences on boundary layer structure and plume dispersion calculations. Three meteorological data sources are evaluated to establish whether there are viable alternatives to the current dependence upon the meteorological pre-processors to estimate boundary layer stability parameters. The first two alternatives are site specific flux profile and sonic anemometer measurements, the last is the use of numerical weather prediction (NWP) data from the Met Office. Analytical techniques were employed to identify and investigate specific conditions in which the uncertainties introduced through both user discretion and model treatment of meteorological inputs, result in ADMS and AERMOD producing disparate predictions. These events may lead to situations where contradictory conclusions could be presented by different model users, leading to wider implications such as the implementation of emergency action plans or granting of a planning consent. This is followed by a probabilistic assessment, using Monte Carlo methods, to determine the range of uncertainty of long and short term ADMS predictions attributed to individual meteorological parameters.

Finally, the last section of the report summarises the main findings of the study with specific attendance to the needs of the model user community. Where possible, methods of best practice for modelling assessments are identified and ideas for further consideration are provided.

2 MEASUREMENT METHODS AND ACCURACY OF METEOROLOGICAL PARAMETERS

Dispersion predictions depend upon the input and treatment of air flow and atmospheric turbulence within the model. Air flow is typically parameterised by measurements of wind speed and direction at 10 m height. Turbulence (the variance of fluctuations in velocity components) is more difficult to parameterise,

with older models such as R91 (Clark, 1979), assigning conditions into one of seven different Pasquill Gifford (PG) stability categories. ADMS and AERMOD offer more continuous coverage of conditions using parameters such as the boundary layer height, h , Monin-Obukhov length, L_{MO} , sensible heat flux, $F_{\theta 0}$, and friction velocity, u^* .

Meteorological data required for emergency prediction purposes may simply be continuous and current site measurements of wind speed and direction, and instantaneous observations of cloud cover. Currently, the UK Environment Agency Air Quality Modelling Assessment Unit (AQMAU) recommend using 5 years of representative hourly sequential meteorological records (Shi & Ng, 2002) for dispersion model assessments for annual licensing purposes. This is considered a practical period with which to assess the influence of local climatology and inter-annual variability on predictions of annual averages and peak hourly concentrations.

Climatological records can be manipulated for input to ADMS or AERMOD. The Met Office provide datasets from UK airports, military airfield sites and Met Office Regional Centres as well as smaller observing sites, which comprise of hourly averages from automatic instruments with additional hourly observations of cloud cover. Similar datasets are provided by ADM Ltd, the UK suppliers of Breeze meteorological data which can be supplied in AERMOD or ADMS format upon request. These records may be spot measurements on the hour, averages over the hour, or a mixture of both. Further information regarding the dataset can be requested at the time of purchase.

The measurement methods and accuracy of parameters are considered in the following sections. The accuracy of an instrument measurement is considered to be the amount by which a recorded value deviates from an accepted standard value. Values can be quoted for the individual parameter sensors (ie, a cup anemometer) or as a measurement system accuracy allowing for the limitations of the signal processing and datalogging systems. The US Environmental Protection Agency (US EPA) have reviewed and approved a meteorological monitoring guide (www.webmet.com) recommending system accuracies for in-situ meteorological measurements for general use in air quality models based on digital recording systems and standard averaging times of nominally 1 hour (see Table 1). It is expected that these system accuracies are typically obtained by the systems used to collate Met Office and ADM Ltd datasets and also by well managed independent measurement sites. The authors are unaware of any equivalent document designed for UK air quality modellers, however the Met Office provide recommendations for the minimum instrument specifications required for a UK climatological station (www.metoffice.gov.uk) and the World Meteorological Office publish a Guide to Meteorological Instruments and Methods of Observation detailing the basic standards of instruments and observing practices. In addition, British Standards exist for the specification of meteorological thermometers and aspirated hygrometers (BS 692:1990, BS 5248:1990) as do guidelines for the acquisition and management of meteorological precipitation data (BS 7843:1996).

2.1 Ringway 2000 meteorological data

Data from Ringway, Manchester for the year 2000 has been used frequently within this study to demonstrate the effects of uncertainty of meteorological data treatment within ADMS and AERMOD. A preliminary review of this dataset highlighted a number of interesting issues which may influence model predictions.

The data was purchased via the Met Office web site in hourly sequential ADMS format, and contained Julian day, time of day, near surface air temperature, wind speed and wind direction at 10 m, precipitation, observed total cloud cover and relative humidity. It was noted that the wind speeds increased in steps of 1 knot/sec (approximately 0.5 m/s), hence records jump discontinuously from 0.5, 1, 1.5, 2.1, 2.6, 3.1, 3.6, 4.1, 4.6, 5.2, 5.7, 6.2, 6.7 m/s and onwards. This is presumably due to the Met Office storing climatological records of wind speed to the nearest knot, however this resolution is well outside the system accuracy of 0.1 m/s quoted by the US EPA, and it is expected that the majority of recently upgraded Met Office sites routinely measure wind speed with a greater resolution than 0.5 m/s. Wind directions are provided to the nearest 10° sector, again, the standard for climatological purposes, this is comparable to the ±5° system accuracy in Table 1. Temperature is reported to the nearest 0.1°C and relative humidity to the nearest 0.1%, these resolutions are high in contrast to the expected system accuracy for these measurements as might be expected from expert siting. A higher than expected frequency of very stable conditions (13% PG category G) was observed, which was also apparent in several other statistically binned ADMS meteorological files provided to WSC by the Met Office. Table 2 also displays boundary layer heights for Category A that are lower (average height of 542 m) than less unstable categories (average height of 687 m for Category C), perhaps due to lighter winds occurring in these extremely unstable conditions.

2.2 Wind field

The wind field is commonly measured as scalar components of speed and direction. These are used within dispersion models to determine the speed and direction in which a plume travels. They are also used to estimate boundary layer parameters, such as friction velocity, and provide the basis for vertical profiling of parameters in ADMS and AERMET (the meteorological pre-processor used in the AERMOD system).

Low wind speeds give rise to additional uncertainty, both due to their effect on the dispersion of a plume but also resulting from their treatment within the dispersion model. The US-EPA recommend that wind speed sensors used for dispersion modelling assessments should have a maximum start up threshold of 0.5 m/s, and an accuracy of ±0.25 m/s at low wind speeds such as 1 m/s (www.webmet.com/met_monitoring). Most modern cup anemometers qualify within these bounds with a typical measurement accuracy of 0.1 m/s. Data

provided by the Met Office typically includes wind speeds down to 0.5 m/s (1 kt), although it is expected that data provided from sites with older instruments may be limited to 1 m/s (2 kts) and above. Wind direction, typically measured with a potentiometer wind vane, is generally reported in dispersion model datasets to the nearest 10°, while instrument accuracy might typically be $\pm 2^\circ$ and system accuracy of $\pm 5^\circ$. Use of wind speed measurements at release height and the input of measured standard deviation of the wind direction (σ_θ) can improve model predictions of lateral dispersion, particularly for users of R91 type model codes (Hill et al, 2001).

2.3 Temperature and relative humidity

It is assumed that resistance temperature detectors (RTDs) are used to provide input to the ADM Ltd and Met Office datasets, these typically have an instrument resolution of 0.1°C and accuracy of ± 0.1 to 0.3°C. System accuracy is likely to be poorer than instrument accuracy due to variation of air flow and shading influences associated with different sites and systems, however careful siting and shielding can ensure accuracies with the US-EPA recommendation of $\pm 0.5^\circ\text{C}$ (Table 1).

Relative humidity (RH) sensors provide a balance of actual vapour density to saturation vapour density at the same temperature. Measurement of temperature and RH together allow the determination of vapour density which can be employed within the model pre-processors. The standard reference heights of measurements of RH and temperature are assumed to be sufficiently similar (within 1 m) within different models such that they will contribute little uncertainty to model formulations of profiles and predictions.

Temperature and humidity values influence plume rise, plume visibility, and to a lesser extent, mixing height and boundary layer parameter calculations. Temperatures are reported in met datasets to the nearest 0.1°C, RH to the nearest 0.1%, however system accuracies are expected to be poorer. Despite this, the overall influence of temperature and humidity inputs on dispersion predictions is expected to be low compared to the stronger influences of other input parameters. One condition where ambient temperature might strongly influence predictions is when emission temperatures fall below ambient temperatures and plume sinkage may occur.

2.4 Precipitation

Deposition of soluble pollutants will be strongly influenced by the frequency and strength of precipitation. Tipping bucket rain gauges are typically used to obtain rainfall records, these usually have a measurement resolution of between 0.1 to 0.2 mm/hr. The accuracy of the instrument is somewhat dependent upon its placement, and it is assumed that climatological records are obtained from sites

suitably positioned to be protected from strong winds in order to avoid spurious tipping.

2.5 Cloud cover

Total cloud cover is recorded in oktas (eighths of sky covered) by the Met Office weather observers as part of the standard observing routine. The requirement to discretely band the amount of cloud can lead to bias in the records, for example the frequency of records giving 1 and 7 oktas may be enhanced due to the observers caution in recording totally clear and totally overcast skies as per their observing instructions. This is apparent in the analysis of cloud records from Ringway in 2000 (see Figure 1). It is unavoidable that observations of cloud cover in the hours of darkness contain an additional uncertainty due to the limitations of the human eye, and typical accuracy of ± 1 okta in day time may increase to ± 2 to 3 oktas overnight.

Cloud observations are gradually being replaced with cloud measurements as the UK Met Office weather stations become increasingly automated. Time series data from laser cloud base recorders (LCBRs) can be processed to provide measurements of cloud height and cloud amount using Sky Condition Algorithms (SCAs). Although these measurements are less susceptible to reduced accuracy during night time conditions, this cloud data also has its limitations. The instrument is designed to view only the zenith of the sky, and does not detect the presence of an invading cloud bank until it reaches overhead. Other developing methods for measuring cloud cover digitally (and then processing into oktas of cloud) include the routine processing of images from an all sky camera. It is possible that these developing methods of cloud cover measurement may supersede manual observations in the future, however, at present we are left with reducing coverage of cloud observations over the UK and no immediate alternative measurement routinely available.

ADMS datasets include values of total cloud cover and do not provide information detailing cloud level. It is possible that a record of 7 oktas cloud corresponds to 7 oktas high level fine cirrus cloud which might exert a lesser influence on surface fluxes than 7 oktas of dense low level stratocumulus. Models such as the Danish dispersion model, OML (Olesen & Brown, 1992), which sits in the same class of models as ADMS and AERMOD, use a heat flux scheme described in Bercowicz & Prahm (1982) and Nielsen (1981) that calculates heat flux allowing for cloud height.

2.6 Solar radiation

Solar radiation can be used within ADMS as an alternative or in addition to cloud cover, although solar radiation measurements from Met Office sites are not routinely included in datasets provided to dispersion modellers. World Meteorological Office second class standard pyranometers are typically adequate

for measuring solar radiation for dispersion modelling purposes (matching the 5% system accuracy acceptable to the US EPA). These are more affordable instruments (~£500) than those matching more exacting standards, and they are regularly included within a standard automatic weather station instrument suite. Solar radiation data is of no use during periods of darkness, instead ADMS reverts to using a default cloud cover value of 5 oktas within its algorithms during these conditions.

3 REPRESENTATIVITY OF METEOROLOGICAL PARAMETERS

The temporal and spatial representativity of meteorological input data is an issue often overlooked by the dispersion model user when considering the uncertainty of overall model predictions. Purchasers of met data for model use can usually obtain a certificate of representativity from the supplier upon request, determining the dataset as the 'most representative' for the emission site in question. A more appropriate label might be 'best available' dataset, as due to limited appropriately measured and formatted data, the closest meteorological sites can be significant distances from the emission site of interest.

This chapter reviews the meteorological input routinely used by modellers and aims to highlight their limitations and inaccuracies. There are obvious difficulties in setting objective criteria to determine whether a met site is representative of an emission site. Distance from the emission site is arguably the most important factor, in order to match the timing of similar air flow over both sites. Length of a data period, local terrain and surface characteristics, coastal influences, and the 'age' of the supplied data are all issues that should be considered on a site by site basis. In reality, wind fields and atmospheric stability will vary with height, location and time due to the localised influences, synoptic weather patterns and stochastic variability. The amount of variation will depend, in part, on the averaging time of the recorded value.

The length of the data period used in a dispersion model assessment should be considered as fit for purpose by the user. Guidance on this decision is available from regulators, for example, the US EPA recommend the use of 5 years of National Weather Service (NWS) data or at least one year of site-specific data within modelling assessments. The AQMAU (UK Environment Agency Air Quality Modelling Assessment Unit) consider 5 years of hourly sequential data to be appropriate for assessments of industrial releases. This period is deemed sufficient to represent the temporal uncertainty associated with annual average and peak concentrations predicted for a point source emission. A recent release of new technical guidance for local authorities regarding air quality management (LAQM TG03, 2002) reviews a variety of studies regarding inter-annual variability and summarises with the suggestion that the use of 2 different met years should give no more than a 30% difference in model predictions of both annual and short-term percentiles. Site specific meteorological data is used

infrequently by the UK Gaussian dispersion modelling community due to industrial monitoring sites generally lacking a sufficient instrumentation to provide a full input dataset. The best practice for statistical binning of meteorological data and its portability have also been subjects of ADMLC research (Smith, 2000).

There is a continuous development of flow and turbulence characteristics during the passage of air over an emission site as the influence of previous land surfaces and topography takes effect. Air flow is also subject to the sometimes abrupt force of synoptic weather systems such as depressions and associated frontal activity. Emission sites located within the influence of a local coastline might also be likely to experience rapid and frequent changes in wind field and stability on both a vertical and horizontal scale. The magnitude of this variability will not be constant, changing on both a spatial and temporal scale. The most rapid changes will be associated with frontal systems that might alter wind direction and speed rapidly within a one hour period, however, for most synoptic conditions the passage of weather systems is sufficiently slow such that their contribution to the uncertainty of model predictions is limited.

The issue of representativity of parameters throughout the vertical height of the boundary layer has been addressed to a limited extent within AERMET. AERMET was designed to accept upper air measurements of temperature, wind speed and direction from radiosondes as well as hourly NWS data and/or site specific data, thus increasing the spatial representativity of input data. Currently, upper air data for the UK is not available for routine use in AERMET, hence providers of AERMOD user interfaces within the UK have incorporated an estimation tool into their model interface that calculates boundary layer parameters using Monin-Obukhov similarity theory. ADMS relies on the calculation of stability corrected vertical profiles using surface based measurements only, whilst R91 recommends using 10 m wind speed or correcting winds to 10 m values using a power law approximation for on axis calculations and does not account for the vertical variation in turbulence. Ideally, meteorological data should be recorded and stored as 10 minute average data for emergency purposes, such that the latest trends are identified prior to running model scenarios. Model users attempting to determine implications of emergency scenarios might also benefit from considering shorter model averaging times, of the order of 10 minutes, to capture these infrequent but significant events. Users of R91 based codes should carefully consider the vertical representativity of wind speed input as Lowles (2002) observed significantly improved performance when using wind speed at release height rather than the default 10 m input. Sites with elevated stacks (significantly above the standard wind speed measurement height of 10 m) may be subject to increased uncertainty than those with lower emissions, particularly in conditions where the stack height is significant compared to the boundary layer height, or where the boundary layer structure is stratified.

In reality, stratified flow is a common phenomena, and stack emissions may be exposed to multiple influences from weak jets and elevated minor inversion layers. These conditions cannot be resolved from surface measurements, neither

can remote radiosonde measurements resolve locally induced irregularities in boundary layer behaviour, highlighting a major limitation of Gaussian steady-state models. The use of dynamic modelling may present less modelling constraints, however, the uncertainty of the predictions may remain similar where the stochastic nature of turbulence is the dominant contributor to overall uncertainty.

The degree of representativity of met data from a remote location for use at an emission site is dependent upon the distance between locations, the similarity in terrain and the surface roughness of the surrounding area. Within the US-EPA guidance, the complexity of the terrain is considered with regard to stack top and plume height. Terrain is classed as 'simple' if below the stack top height, 'intermediate' if between the stack top and plume height and 'complex' if above the plume height. The UK Environment Agency guidance leaves the decision to consider the significance of terrain to the modeller, requiring a justification of the choice of modelling scenario. CERC (2001) recommend using terrain grid files in ADMS where the local gradients exceed 10%. Where the emission site is located in complex terrain, a terrain file can be incorporated into the models to assess flow fields over the model domain, which will in turn influence local meteorological parameters. Where terrain is sufficiently complex, and meteorological datasets sufficiently sparse, it might be most appropriate, where practicable, to set up a tower to record measurements close to the emission source at plume height. In reality, siting of instrumentation is usually a compromise between practicality and usefulness. A site evaluation should be undertaken to consider the most appropriate placement of equipment if that option is to be pursued. Alternatively, dynamic modelling may be required to create diagnostic wind fields over the area of interest.

3.1 Low wind speeds and calm conditions

Peak concentration events are often predicted to occur in light wind speed conditions. Treatment of light wind conditions within models should therefore be as realistic as possible to account for these occasions. Models typically have a limiting value of wind speed below which dispersion calculations are not completed. ADMS does not predict downwind concentrations for any hour in which the wind speed is below 0.75 m/s. AERMET uses a threshold of $2^{1/2}\sigma_{v_min}$, equivalent to 0.28 m/s, below which no dispersion calculations will be performed (EPA, 1998). AERMET was designed to receive NWS met data as hourly input, in which the lowest reported wind speed is 1 m/s. This is in contrast to the Met Office datasets supplied in ADMS format, which include minimum values of 0.5 m/s. ADMS datasets can be converted within Lake's AERMET user interface to SAMSON format (similar to that of NWS) hourly data. Predictions using this data will be completed for all available datapoints unless wind speeds read below 0.28 m/s.

Using Ringway 2000 data as an example, ADMS will not predict concentrations for 413 hours of data (3 data gaps, 208 calm measurements where $u=0$, and

202 hours where wind speed records are 0.5 m/s). AERMOD will not calculate concentrations for the 3 data gaps and 208 hours of calm measurements, but will predict for hours where wind speeds are 0.5 m/s. Where site specific meteorological data are input to AERMET, a minimum threshold value of wind speed can be set, this should match the threshold start up speed of the site anemometer. The frequency of calms and the different treatment of low wind speeds between models highlight the issue that model assessments, for both standard and emergency purposes, should cautiously consider the treatment of low wind speed data and its impact on the reported predictions.

3.2 Data gaps

Data purchased from the Met Office and ADM Ltd is normally provided with greater than 99% coverage, with typically 2-3% calm conditions. The user is provided with no information regarding any data filling procedures (eg, interpolation between hours or concatenation of data from two sites) that may have been carried out prior to purchase. The US EPA recommend that meteorological datasets should be a minimum of 90% complete, allowing a maximum of 10% data to be substituted for use in the dispersion model. They recommend filling single hour gaps using persistence or interpolation techniques, and suggest that using these techniques for longer periods will result in 'moderate probable error', as will substituting data from a similar (surface-specific) site. 'High probable error' is expected from using a close but dissimilar location, monthly average, simulated or 'dummy' data. If met data is obtained on site, careful processing following current guidelines should be completed. When calculating peak percentile values the model's treatment of missing data should be acknowledged. For example, the 99.7th percentile value might be taken as the 26th highest value for a full year of data (8760 hrs) but would be the 25th highest hour for 8300 hrs of data.

3.3 Atmospheric stability

R91 based Gaussian models use time of day, cloud cover and wind speed parameters to determine the influence of stability on dispersion using the simple discrete PG stability category scheme where Category A is extremely unstable and Category G is most stable. Environmental assessors required to determine the impacts of an accidental release can use nomograms from Clarke (1979) to estimate a stability category. A typical daytime accuracy of ± 1 okta can result in predicted stability differing by ± 1 stability category, although in low wind speeds and during night-time periods, situations may occur where predictions differ by ± 2 categories.

Cloud cover is the most typical input used to calculate further boundary layer parameters in more modern Gaussian models such as ADMS and AERMOD, hence the models are similarly susceptible to the inaccuracies of cloud observations.

Friction velocity, u_* (m/s), represents the turbulent eddy velocity, and sensible heat flux, $F_{\theta 0}$ (W/m^2), represents the exchange of sensible heat over the ground surface, positive values representing net output from the ground, ie, typical in convective conditions. The Monin-Obukhov length, L_{MO} , (m) represents the height at which equal magnitudes of turbulent kinetic energy are generated (or consumed) by convective and mechanical forces; this is dependent upon $-u_*^3/F_{\theta 0}$. In convective or unstable conditions L_{MO} is negative, with its magnitude being a measure of the height above the surface at which thermally induced turbulence, the convective motion, is more important than mechanical turbulence generated by friction at the surface. In stable conditions, L_{MO} is positive and gives a measure of the height above the surface where vertical turbulent motion is greatly inhibited by stratification. Steady state Gaussian models assume a single value of u_*^3 , $F_{\theta 0}$ and L_{MO} as representative over the surface model domain for the length of averaging time (typically one hour). In reality, these parameters and vertical profiles of temperature, wind speed and direction will evolve continuously over space and time as they react to surface and synoptic influences.

3.4 Surface energy balance parameters

The net radiation balance at the surface is determined in part by the fraction of radiation reflected from the surface. This reflection coefficient, or albedo (r), is dependent upon surface characteristics and changes on a daily and seasonal scale. ADMS defaults to a constant value of 0.23 for albedo throughout the year, although it is possible to input hourly values where they are known. Using this default value may result in under-estimating the frequency and magnitude of stable conditions for sites that have significant periods of snow cover. The surface radiation balance is also strongly influenced by the latent heat flux which is dependent upon the amount of moisture present at the surface. The availability of moisture at the surface will alter significantly over space and time depending upon surface characteristics and the intermittency of precipitation. This will contribute to uncertainty in partitioning of heat flux between latent and sensible flux and will therefore add to uncertainties in sensible heat flux estimates. Although the influence of meteorological uncertainty on deposition predictions has not been considered in detail within this report, it is noted that the inherently large spatial and temporal variation of rainfall will lead to large uncertainty on deposition predictions over a model domain when using a spot measurement of precipitation.

ADMS uses the modified Priestley-Taylor parameter (α) to represent the fraction of surface moisture available for evaporation. This is defined by

$$\alpha = \frac{1 + \gamma/S}{1 + \beta} \quad \text{Equation 1}$$

where the psychrometric constant, $\gamma=c_p/\lambda$, with λ being the specific latent heat of vaporisation of water, c_p the specific heat capacity of water, s the rate of change of saturation specific humidity with temperature, and β is the Bowen ratio, the ratio of sensible to latent heat flux. A default value of $\alpha=1$ ($\beta=0.6$), typical for moist grassland, is used within ADMS which may under-estimate moisture availability over nearby bodies of water or after prolonged periods of precipitation (particularly over areas susceptible to flooding) and over-estimate availability during dry conditions. This could lead to corresponding significant over and under prediction of sensible heat flux. The AERMET user is requested to specify a surface characteristic for the emission site, eg, cultivated grassland, for which seasonal values of albedo, Bowen ratio and surface roughness, z_0 are then provided. Surface characteristics can be input on a sector based level, increasing the spatial resolution of these parameters beyond that of single input default values in ADMS. The influence of albedo and surface moisture balance on dispersion predictions is investigated within sections 6 and 7 of the report.

3.5 Surface roughness

Roughness length, z_0 , represents the aerodynamic effects of surface friction and is physically defined as the height at which the extrapolated surface layer formula (eg, log law in neutral) goes to zero. This value is an important parameter used by meteorological pre-processors to interpret the vertical profile of wind speed and estimate friction velocities which are in turn used to define heat fluxes and turbulence level. Typically a single value of z_0 is input to represent the emission site in ADMS and R91 models, with ADMS offering the option of inputting an additional value for the met site where it is considered 'non-representative' of the emission site in question. It is also possible to create a z_0 grid over the ADMS model domain, although it is believed that few users utilise this capability for routine assessments. Use of a z_0 grid has the additional advantage of determining the influence of surface roughness on boundary layer structure both up and downwind of the source. Seasonal and sectoral values are assigned to the emission site within AERMET based upon the user's choice of surface characteristics. Roughness length at the meteorological data site is determined from flagging the site as 'urban' or 'rural'. It is also possible to input hourly values of z_0 to AERMET through the meteorological data file.

Roughness length will vary in space and time during the passage of a plume from an emission point, depending upon the fetch over which the air has previously travelled. A detailed study to quantify the influence of using single value z_0 , sector specific or grid level values is beyond the scope of this document, however interested readers are directed towards Hanna & Britter (2002) for further recommendations on appropriate roughness lengths for complex locations. More complex treatment of roughness length could potentially add significant financial and time constraints to assessments, if for example, a roughness length grid was deemed necessary. In practice, individual sites will need to determine whether or not this is necessary for their requirements.

4 TREATMENT OF METEOROLOGICAL INPUT WITHIN ADMS AND AERMOD

4.1 Meteorology

One of the major advances of ADMS and AERMOD, compared to the models they were developed to replace (R91, ISC3), is in the treatment of the Planetary Boundary Layer (PBL). The growth and structure of the PBL is driven by fluxes of heat and momentum, which in turn depend upon local surface effects such as the surface roughness, reflectivity and moisture levels.

ISC3 and similar 'older generation' Gaussian models, such as R91, are based on Pasquill-Gifford stability categories. The stability of the atmosphere is divided into generally seven discrete regions (Pasquill-Gifford stability categories A to G) dependent upon wind speed and surface heat flux. Dispersion characteristics are then defined for each category. Thus, a slight variation in meteorological conditions can result in a change in stability category and consequently significant variation in model concentration predictions.

The so-called 'new generation' models, such as AERMOD and ADMS, characterise the boundary layer structure using continuous parameters such as the boundary layer height, h , and the Monin-Obukhov length scale, L_{MO} . Similarity profile relationships are used to calculate the boundary layer structure in terms of two variables, z/L_{MO} and z/h , where z is vertical height. This allows for the variation of boundary layer properties with height, a crucial difference from the Pasquill-Gifford formulation in which boundary layer properties only vary discretely with stability category. It is difficult to make exact comparison between the two schemes, as the Pasquill-Gifford categories are not a simple function of z/L_{MO} , particularly under stable meteorological conditions (CERC, 2001).

While AERMOD and ADMS both use equivalent concepts derived from the same meteorological research base in determining the stability characteristics of the PBL flow, the methods and parameterisations used do vary. Hall et al (2000) reported significant variations, factor of 2 or 3, in the predicted L_{MO} and h between the ADMS and AERMOD meteorological pre-processors using selected single meteorological conditions from hourly sequential meteorological data collected at Lyneham, UK, during 1995.

The estimation of the sensible heat flux, $F_{\theta 0}$, is critical in determining both L_{MO} and h . In both models the boundary layer depth in unstable conditions is determined from the boundary layer's past history, growing as a result of the daytime sensible heat flux. However, the prediction of $F_{\theta 0}$ can have a large uncertainty resulting from the estimation of variables in its formulation, primarily from the estimation of the available surface moisture which determines the partitioning between latent and sensible heat flux. Thus, both L_{MO} and h depend upon variables that are not routinely determined, and are therefore susceptible to higher uncertainty.

Generally, the differences are not as serious as might be first thought, with the 'new generation' models being a significant improvement on the 'older generation' models due to their ability to incorporate variations in PBL characteristics with height. However, for elevated or buoyant sources estimation of the boundary layer height can be critical, with both the new and older generation models using h to determine how much of a plume penetrates the boundary layer and how much remains within the boundary layer, in addition to placing a limit on the vertical spread.

In their response to the report by Hall et al (2000) the developers of ADMS commented in relation to these variations: "In our view the differences are not surprising and reflect real uncertainties in predicting surface heat flux and boundary layer depth." (Carruthers et al, 2001). While reducing the uncertainty in predicting such critical parameters would be desirable, a degree of uncertainty exists in the data used for developing the models as well as in the estimation of the model input parameters. Thus uncertainty in these parameters is unlikely to reduce below certain levels.

It is not the intention of the authors to determine whether one model outperforms the other. Even an extremely rigorous investigation into the performance of the meteorological pre-processors of both ADMS and AERMOD is unlikely to determine most realistic performance as it would probably be impossible to obtain a suitably extensive and reliable data set on which to base such work. Thus, in looking at the processes of both models it is currently only possible to investigate the disparity between the models and the resulting differences in the final dispersion predictions. In doing this we consider Version 3.1 of ADMS (CERC, 2001) and Version 02222 of AERMOD (Cimorelli et al, 2002). It should be noted that as this latter document was not available until well after the commencement of this project, an earlier document (Cimorelli et al, 1998) was relied upon for much of the model technical detail. Discussions and conclusions within this report are not altered by the publication of the more recent AERMOD user guide.

4.2 Meteorological pre-processors

Both AERMOD and ADMS employ meteorological pre-processors whose role is to determine meteorological parameters necessary for estimating profiles of wind, turbulence and temperature from standard meteorological measurements. The standard meteorological parameters taken as input do differ, although both pre-processors currently require a minimum of:

- wind velocity at a reference height, u_z ,
- wind direction at a reference height, ϕ_z ,
- temperature (Dry Bulb) at a reference height, T_z , (required in AERMOD but not essential in ADMS) and

- cloud cover, Cl , (or solar radiation, F_{θ_0} , or $1/L_{MO}$ can be used as alternatives within ADMS).

The meteorological pre-processors also require surface parameters such as surface roughness, z_0 , albedo and either a Bowen ratio or a modified Priestley-Taylor parameter in conjunction with location and time information. Originally, AERMET, also required a pre-dawn upper air sounding. However, due to the limited availability of such data, except in North America, a boundary layer height estimation method is now incorporated into the proprietary user interfaces developed to enhance the operation of AERMOD. The interface used in this project was that developed by Lakes Environmental (Thé et al, 2000) which in unstable conditions uses a boundary layer height estimation technique adapted from Thomson (1992, 2000) which was developed for ADMS (Thé et al, 2001).

The surface parameters provided by the meteorological pre-processors, to the boundary layer structure algorithms, also differ, although the main boundary layer parameters, listed below, are common to both pre-processors:

- Monin Obukhov Length, L_{MO} ,
- Friction velocity, u_* ,
- Surface roughness length, z_0 , (input directly)
- Sensible heat flux, F_{θ_0} ,
- Convective velocity scale, w_* , and
- Boundary layer heights, h ,

(NB: AERMET outputs estimates of both the convective, h_{ic} , and mechanical, h_{im} , mixed layer heights).

The ADMS meteorological pre-processor output includes all measured inputs, plus additional near surface parameters of specific humidity and latent heat flux. The maximum turning of the wind with height, the temperature step across the elevated inversion and the buoyancy frequency and relative humidity lapse rate above the boundary layer are also estimated by the ADMS meteorological pre-processor.

Assuming the minimum meteorological input data listed above (ie, u_z , ϕ_z , T_z and Cl), which are generally standard in UK, the overall approach taken by the two pre-processors in parameterising the boundary layer is broadly similar, although, as with the input and output data there are subtle differences. Both use the solar angle, determined from time of day and time of year, cloud cover and albedo, to estimate the net radiation. If the net radiation is positive, the PBL is defined as convective, with both using energy balance principles to estimate the sensible heat flux, however, the equations for estimating F_{θ_0} do differ slightly. AERMET uses the equation of Oke (1978) while ADMS uses the parameterisation of Holtslag and Van Ulden (1983). The parameterisations differ by the amount of

20α , where α is the modified Priestley-Taylor parameter used in ADMS. Using the ADMS default value of $\alpha=1$, this suggests AERMET will give sensible heat flux estimates 20 W/m^2 higher than those predicted by ADMS. While this difference is generally of little significance, when the net radiation is low this amount can be a substantial proportion of the total sensible heat flux. The difference is likely to be most significant in the hours near dawn and dusk or highly overcast conditions when the sensible heat flux is low. It is possible one pre-processor may classify the stability as unstable while the other could give a stable classification.

Under convective conditions both models use the sensible heat flux (F_{00}) estimation to compute u_* and L_{MO} , based on the methods of Panofsky and Dutton (1984). As u_* and L_{MO} are interdependent this requires an iterative procedure. Both models also use F_{00} , in conjunction with the potential temperature gradient, to calculate the time evolution of the convective boundary layer throughout the day, and thus the estimation of the boundary layer height, h . AERMOD also calculates the boundary layer height due to mechanical turbulence, and when it is greater than that due to thermal convection (under weak convective conditions) it is used in preference. ADMS tries to incorporate the affect of mechanical turbulence directly into its boundary layer growth formulae.

The original AERMOD method for convective conditions is based on simple one-dimensional energy budget principles, which uses the early morning potential temperature sounding in conjunction with the time varying sensible heat flux. However, this method is not suitable for use in the UK as routinely measured potential temperature sounding data are not available. As mentioned above, to enable more global use, a boundary layer height estimation method is now incorporated into the proprietary user interfaces developed to enhance the operation of AERMOD. A comparison between the use of sounding data and the estimation method within the Lakes Environmental version of AERMOD (Thé et al, 2001) indicated the estimation method predicted the height of the boundary layer to be larger by nearly 50% on average. However, for stacks up to 60 m this was found to have only a minor influence on the mean and peak concentration predictions. For taller stacks and highly buoyant plumes that may rise to the top of the boundary layer or penetrate the elevated inversion, the differences may become more significant.

When the net radiation is negative the PBL is defined as stable. Under stable conditions neither model uses energy budget considerations, preferring instead to use semi-empirical methods for estimating u_* and L_{MO} . The eddy temperature θ_* , is estimated from the cloud cover following Van Ulden and Holtslag (1985). In stable and neutral boundary layers, in which only mechanically generated turbulence exists, both ADMS and AERMOD use u_* , L_{MO} and the Coriolis parameter, f , to estimate the boundary layer height (Nieuwstadt, 1981; Zilitinkevich, 1972; Venkatram, 1980). To prevent extreme values occurring, both models have upper limits of 4000 m on the boundary layer height, while ADMS also has a lower limit of 50 m.

4.3 Boundary layer structure calculations

Following the estimation of the primary boundary layer parameters within the meteorological pre-processors, as described above, both models then proceed to use similarity relationships, in conjunction with the boundary layer parameters, to compute vertical profiles of:

- mean wind speed, $u(z)$,
- potential temperature, $\theta(z)$, and
- vertical and horizontal turbulence components, $\sigma_w(z)$ and $\sigma_v(z)$.

Both ADMS and AERMOD use forms of stability correction functions based on Panofsky and Dutton (1984) in convective conditions. In stable conditions AERMOD uses those of Van Ulden and Holtslag (1985) while ADMS uses Holtslag and de Bruin (1988). ADMS utilises three sets of turbulence parameterisation schemes as described in Hunt et al (1988) (an internal CERC report) depending upon h/L_{MO} . Changes in the parameterisations cause discontinuities at the boundaries of the defined stability regions, while AERMOD uses a continuous turbulence parameterisation scheme throughout the stability range (Cimorelli et al, 2002).

One of the primary differences between the two models in determining the structure of the boundary layer is the ability of AERMOD to consider on-site measurements in addition to the standard meteorological data. Although several UK industrial sectors have a growing requirement to obtain site specific meteorological data to fulfil environmental regulations, at present it is understood that these data are not routinely incorporated into dispersion model input, except for emergency purposes, perhaps due to data archiving and processing difficulties. Thus, the inclusion of site specific data is not the standard mode of operation in the UK, even for large industrial sites.

4.4 Plume dispersion

New generation atmospheric dispersion models, such as AERMOD and ADMS, are also often referred to as modified Gaussian models. Like the older generation models (ISC3 and R91) they generally use a simple Gaussian form to describe the plume spread and determine concentrations. However, the application of the Gaussian model and the determination of the dispersion coefficients is more sophisticated in the new generation models.

The older generation Gaussian dispersion models were very simplistic, not properly accounting for the physics of real atmospheric flows and dispersion phenomena. They assumed the plume travelled horizontally, with the lateral and vertical spread determined solely by the atmospheric stability class in a step function. Their only additional feature was the inclusion of the reflection term to account for the plume's interaction with the ground and inversion layer. Features

such as the variation of turbulence with height and within an atmospheric stability regime are not addressed in such models. More complicated processes such as the effect of complex terrain, the non-Gaussian nature of convective plumes, plume lofting and fumigation of elevated plumes within convective boundary layer (CBL) flows are not routinely considered within R91 based models.

An area in which the new generation atmospheric dispersion models vary significantly from the traditional Gaussian models, is in their approach to dispersion in the CBL. In the neutral and stable boundary layers (NBL and SBL) the distribution of the turbulent velocities is Gaussian in nature, ie, normally distributed about the mean, with, for the vertical velocity component, updrafts and downdrafts occurring for equivalent amounts of time. However, the vertical velocity distribution in a CBL is not Gaussian in nature. Downdrafts are more prevalent and with correspondingly weaker velocities than the less frequent updrafts of higher velocity to ensure mass continuity. In addition, convective circulations within the CBL fill the space available, with the dominant scale of the turbulence being of the order of the depth of the boundary layer. Thus large eddy time scales of the order 10 to 20 minutes are typical in strongly convective conditions.

This has a significant and unusual effect on the dispersion of plumes released into the CBL. The point of maximum concentration of a passive plume released close to the surface lifts from the ground and gives rise to an elevated locus of maximum concentration. In contrast the point of maximum concentration of a passive plume released from an elevated source will descend until it impinges on the ground, where it will remain for a considerable time before it ascends in a manner similar to a surface source. This behaviour is contrary to the traditional view of a Gaussian plume moving downwind and spreading vertically and laterally from a fixed height, and can produce significantly higher concentrations at the surface than predicted by standard Gaussian plume models. Another complication is that due to the large time scales of the convective motions, a mean hourly concentration, as generally predicted by atmospheric dispersion models, is often not an appropriate time scale to obtain a stationary average. In practice, under strongly convective conditions hourly average concentrations will vary significantly, with a minimum period of several hours required to obtain close to a stationary average.

AERMOD's dispersion algorithms for the CBL are based on Gifford's (1959) meandering plume concept in which a small 'instantaneous' plume wanders due to the large eddies in a turbulent flow. The instantaneous plume is assumed to have a Gaussian concentration distribution about its randomly varying centreline. The mean, or average, concentration is calculated by summing the concentrations due to all the random centreline displacements computed from the probability density functions (pdfs) of the vertical and lateral velocities.

Similarly ADMS uses a simple Gaussian formulation for stable and neutral boundary layer conditions. However, for the CBL, ADMS uses a non-Gaussian or skewed vertical concentration distribution, which ensures that for elevated

sources the locus of maximum concentration descends as the plume moves downwind. In a simple trial the locus of maximum concentration did not appear to rise again after it had reached the ground, although it is claimed it can within CERC (2001).

Like R91 and ISC, ADMS and AERMOD are steady-state plume models designed to apply to releases and meteorological conditions that can be assumed steady over individual modelling periods, generally 1 hour. However, within each period AERMOD can simulate five different plume types depending on the atmospheric stability and the location of the plume in and above the boundary layer as summarised below:

- **direct plume** –remains within the mixed layer initially.
- **indirect plume** – rises and tends to initially loft near the top of the mixed layer before mixing.
- **penetrated plume** – released into the mixed layer but rises to penetrate into the elevated inversion above the mixed layer.
- **injected plume** – where the release height is greater than the inversion height, with the plume released directly into the stable elevated inversion before being entrained into the mixed layer.
- **stable plume** – modelled with the familiar horizontal and vertical Gaussian distribution.

The first four refer to plumes released in unstable surface conditions, while the fifth, as it states, is for stable conditions.

ADMS generally only considers the direct and indirect plumes in the CBL, although if a penetrated plume is allowed to escape the boundary layer it is not re-entrained. Apart from in the specific coastline module, ADMS does not model the re-entrainment of releases that are injected or penetrate above the elevated inversion, back into the mixed layer under unstable atmospheric conditions. For very tall stacks and low boundary layer height convective conditions, this may result in AERMOD predicting higher ground level concentrations than ADMS.

4.4.1 Dispersion parameter estimation

In R91 the lateral and vertical dispersion parameters (σ_y and σ_z respectively) were related directly to the stability category of the atmosphere in a step function. No account of variations resulting from differing plume heights or turbulence levels within stability categories are taken, neither are local turbulence enhancements resulting from buildings or roughness variations considered in most older generation models. New generation models, such as ADMS and AERMOD, use more sophisticated routines for determining the concentration distributions. Dispersion is directly related to the turbulence level and scale of the flow field in which the plume is travelling.

AERMOD incorporates contributions from the individual sources of turbulence resulting from the atmospheric ambient turbulence, plume buoyancy induced turbulence and enhanced turbulence resulting from building wake effects. The total dispersion coefficients, σ_y and σ_z , are calculated from a general expression of the form (Pasquill and Smith, 1983):

$$\sigma_{y,z}^2 = \sigma_{ya,za}^2 + \sigma_{yb,zb}^2 + \sigma_{yd,zd}^2 \quad \text{Equation 2}$$

where, $\sigma_{y,z}$ is the total dispersion in either the crosswind, y , or vertical, z , direction, and σ_a , σ_b and σ_d are the dispersion coefficient contributions from the ambient atmospheric turbulence, buoyancy induced turbulence and building downwash induced turbulence respectively. In the more recent version of AERMOD, which incorporates the PRIME buildings algorithms, building downwash induced turbulence is treated separately. Similar ideas of incorporating different individual contributions to dispersion are employed by ADMS, although, as with the models throughout, the methodologies differ in their more detailed application. Although none of the individual contributions to the total dispersion should be ignored, it seems more appropriate in the context of the current work to concentrate on the contributions that result from atmospheric flow and turbulence.

Turbulence levels within the atmospheric boundary layer are known to vary significantly with height, with the strongest variation near the earth's surface and under stable and neutral conditions. As a result, the dispersion induced by the ambient turbulence also varies with height. With the ability to estimate the vertical structure of the PBL, AERMOD and ADMS are able to utilise an applicable turbulence level at the plume height and atmospheric stability when estimating spread parameters for use in the dispersion equations. Calculation of the dispersion coefficients due to ambient atmospheric turbulence generally follows a statistical theory equation of the form:

$$\sigma_{y,z} = \sigma_{v,w} t (1 + f n_{y,z} (t/T))^{-p} \quad \text{Equation 3}$$

Here, $\sigma_{v,w}$ are the lateral and vertical turbulence, t ($=x/u$) is the mean travel time, T a relevant time scale dependent upon the source and atmospheric conditions and p is generally equal to 0.5. This is a somewhat simplified general form of the equations used to calculate the dispersion parameters from the state of the atmosphere, particularly for vertical dispersion in the CBL where a bi-Gaussian approach further complicates the formulation.

The approach to determining applicable parameters, such as turbulence level, wind speed, etc, for use within the dispersion coefficient equations differs significantly between the two models. ADMS typically uses values estimated from the boundary layer structure parameterisation at the mean plume height.

AERMOD uses a more complicated approach based on the concept that the primary region of importance is the one through which the plume travels directly from the source to the receptor. Thus, effective values of the boundary layer parameters are determined by averaging over the region between the plume centroid height and the receptor height.

Under stable and neutral atmospheric conditions, ADMS and AERMOD both use parameterisations based on statistical theory to relate the lateral and vertical dispersion parameters (σ_y and σ_z) to atmosphere turbulence levels (σ_v and σ_w).

As was the case in R91, the ADMS parameterisation is based upon a lateral turbulence-induced dispersion component, σ_{yt} , and a wind direction unsteadiness component, σ_{yw} , following Moore (1976). Thus the total lateral dispersion due to atmospheric flow and turbulence is given by $\sigma_y^2 = \sigma_{yt}^2 + \sigma_{yw}^2$. The directional unsteadiness component, σ_{yw} , is proportional to σ_θ , the standard deviation of the horizontal wind direction. In principle, σ_θ should be determined from 3-minute average wind direction measurements over the modelling period of generally one hour in ADMS, although, typically σ_θ based on 10-minute averages or a parameterisation based on u_{10m} is used. The use of σ_θ based on a 10-minute average would be expected to give slightly lower σ_{yw} and thus dispersion than σ_θ based on a 3-minute average.

Under stable conditions AERMOD includes the effect of the slow lateral plume shift due to shifting wind directions during the modelling period using a meandering plume model as opposed to a direct measurement or estimate of σ_θ .

In determining the turbulence-induced lateral dispersion component, σ_{yt} , from σ_v , both models use parameterisations based on interpolation forms of Taylor's (1921) small and large travel time dispersion relations. Again, the parameterisations differ slightly, with that used in AERMOD being empirically tuned with the full Prairie Grass (Barad, 1958) data set to overcome problems observed with the treatment of lateral dispersion for near surface releases. It is not immediately clear as to how the ADMS parameterisation has developed, with no attribution given in either the User Guide (CERC, 2001) or the Technical Specifications (Carruthers et al, 2000).

In estimating the vertical dispersion parameter, σ_z , under stable or neutral atmospheric conditions both AERMOD and ADMS use different solutions for surface (where shear plays a significant role) and elevated dispersion in conjunction with transitional smoothing functions. Although the basic approach is similar, the parameterisations used differ. For further information the reader is directed to Venkatram (1992), Weil (1985) and Hunt (1985).

In unstable conditions the turbulent component of lateral dispersion, σ_{yt} , is derived from combining both convectively and mechanically generated turbulence. In AERMOD both turbulence components are incorporated directly in the estimate of the lateral turbulence, σ_v , with the final form of the σ_y parameterisation obtained from an empirical fit to the Prairie Grass measurements. An empirical relation is also used to account for variations in release height from that of the Prairie Grass experiments. ADMS independently

calculates a convective dispersion parameter, based on the convective turbulence and the convective velocity and a mechanical dispersion parameter, based on shear-generated turbulence and the shear velocity. The final turbulent lateral dispersion parameter is determined from the combined influence.

In AERMOD the turbulent component of the vertical dispersion, σ_{zt} , during convective conditions is composed of an elevated and surface portion to distinguish between near surface and elevated releases. However, the surface portion, based on Venkatram (1992), contributes to only 10% of the boundary layer height. Thus, only the elevated portion of vertical turbulence is considered throughout the mixed layer region of the boundary layer. A bi-Gaussian pdf formulation, following Weil et al (1997), is used to account for the skewed nature of the vertical turbulence and thus dispersion in the CBL.

ADMS also uses a non-Gaussian pdf to describe the convective component of turbulent vertical dispersion in the CBL. The ADMS formulation is based on the vertical velocity distribution described by Hunt et al (1988). As the form of the ADMS Gaussian plume formulation for the convective boundary layer is not the same as that of the neutral or stable boundary layers, a transitional smoothing formulation is used between neutral and convective dispersion.

4.5 Summary

ADMS and AERMOD, the 'new generation' atmospheric dispersion models developed in the UK and US respectively, incorporate more up-to-date planetary boundary layer and dispersion concepts, with both models bringing improvements over older dispersion models such as R91 and ISC, particularly in relation to:

- the continuous characterisation of the planetary boundary layer through surface fluxes,
- the characterisation of the dispersion parameters in terms of the local turbulence,
- the use of convective scaling and bi-Gaussian vertical dispersion in unstable conditions.

The 'new generation' models were essentially developed from the same research and theory base, although the application of different parameterisations and assumptions results in a number of differences between them. This work has attempted to highlight both the similarities and differences in meteorological modelling approach together with the potential impact on dispersion calculations. The complexity of the model formulations makes it virtually impossible to quantify the impact of the subtle differences on every processed parameter without undertaking an extremely rigorous investigation. Appropriately reliable data enabling such an undertaking is scarce with much of what is available already used in the model development. Section 6 identifies specific occasions

where ADMS and AERMOD model predictions differ significantly due to critical assumptions and differences in model approach highlighted in this section.

5 EVALUATION OF ALTERNATIVE METHODS FOR ESTIMATING BOUNDARY LAYER PARAMETERS FOR DISPERSION MODELS

The majority of routine modelling assessments using ADMS or AERMOD are completed using meteorological data obtained from suppliers such as the Met Office and ADM Ltd. There are few independent sites at which suitable and sufficient measurements are recorded to be used as input to second generation dispersion models. Where on-site data are available, careful consideration should be made of the weather station position with respect to local obstructions to air flow such as buildings and changes in fetch and surface characteristics.

Where on site measurements are used to estimate boundary layer stability, cloud cover or solar radiation is most frequently used to estimate either Pasquill Gifford stability categories or boundary layer parameters such as Monin Obukhov length. Solar radiation measurements give an estimate of the total energy input into the surface energy balance. Assumptions can then be made (within the model pre-processors) of the partitioning between the various loss pathways to derive the emissions of radiation from the surface in the form of sensible heat. This method is of course of little use during overnight periods when the surface energy balance is no longer driven by solar inputs.

Alternative methods, that can be used to directly estimate friction velocities, sensible heat fluxes and therefore Monin-Obukhov lengths, include the use of eddy correlation techniques, using sonic anemometry, and the application of flux-gradient relationships to measured wind speed and temperature profiles. In order that the results of these measurements can be used in dispersion modelling, assumptions of homogeneity in the upwind (fluxes are constant across the upwind fetch) and vertical (measurements are made in a constant flux layer) must be made.

This section reviews the use and uncertainty of these alternative techniques for estimating boundary layer parameters. The issue of measurement uncertainty and uncertainty due to sensor configuration, when using flux-gradient methods is considered in detail. These uncertainties are propagated through the ADMS 3.1 atmospheric dispersion model to investigate their contribution to uncertainty in the prediction of air concentrations. Appendix A provides further background to the flux profile method that has been employed within this section. The use of NWP data as a further alternative data source is also evaluated in Section 5.3.

5.1 Eddy-correlation method

The eddy-correlation method estimates surface sensible heat fluxes directly from turbulent fluctuations in vertical wind speed (w') and the corresponding fluctuations in air temperature (T'). Turbulent fluctuations in the horizontal and lateral wind velocities are denoted as u' and v' and are used to calculate the friction velocity. The sensible heat flux and friction velocity can be determined from the time-averages of these correlated fluctuations.

$$F_{\theta 0} = \rho_a C_p \overline{w'T'} \quad , \quad u_* = [(\overline{u'w'})^2 + (\overline{v'w'})^2]^{1/4} \quad \text{Equation 4, 5}$$

The validity of the above relationships depends on the correct alignment of the sonic anemometer and the selection of a suitably flat site to ensure that $w_{mean} = 0$. Tilt errors have been found by Dyer (1981) to cause an error of approximately 14 % in u_* per degree. In order to minimise the impact of these error terms 2 or 3 dimensional co-ordinate rotations are often performed. Zeller (1993) estimated that in ideal conditions the error in heat fluxes derived using sonic anemometers was of the order of 14 %. This compares with estimates of 20% uncertainty in the derivation of fluxes over extensive Kansas wheat fields by Haugen et al (1971).

5.2 Flux-gradient method

Friction velocities, sensible heat fluxes and thus Monin Obukhov lengths can also be estimated from measurements of air temperature and wind speed at a number of vertical heights using flux-gradient relationships. A commonly used set of equations are:

$$\text{Friction velocity} = u_* = k \frac{\partial u \{z - d\}}{\partial [\ln(z - d) + \Psi_M]} \quad \text{Equation 6}$$

$$\text{Eddy temperature} = \theta_* = k \frac{\partial \theta \{z - d\}}{\partial [\ln(z - d) + \Psi_H]} \quad \text{Equation 7}$$

$$\text{Sensible heat flux} = F_{\theta 0} = -\rho_a C_p u_* \theta_* \quad \text{Equation 8}$$

$$\text{Monin Obukhov length} = L_{MO} = -\frac{\rho_a C_p (\theta + 273) u_*^3}{k g F_{\theta 0}} \quad \text{Equation 9}$$

Where, θ is the potential temperature in degrees Celsius and d is the height of the aerodynamic zero plane. Ψ_H and Ψ_M are semi-empirical stability correction

factors for heat and momentum that have been integrated with respect to height. Errors in the estimation of surface fluxes using the flux-gradient method range between 10-30% (Baldocchi et al, 1988) and are largely due to the empiricism of the factors Ψ_H and Ψ_M . Consequently errors in the determination of boundary layer parameters using these methods are expected to be highest during periods of stability extremes.

A further limitation of the aerodynamic gradient method can occur due to the violation of the constant flux layer assumption. Horst and Wiel (1994) found that fetch to height ratios, representing the uniform upwind distance required for a constant flux layer to extend to a specific measurement height, can be 1000:1 during stable conditions (ie, a measurement at a height of 1 m requires a uniform upwind fetch of 1 km) and up to 200:1 for neutral conditions. As a result, Horst and Wiel (1994) showed that micrometeorological measurements of heat fluxes made using the rule-of-thumb fetch to height ratio of 100:1 could be in error by 20 % for neutral conditions and more than 50 % for stable conditions.

5.2.1 Assessment of the errors in applying flux gradient methods

Flux-gradient methods can be employed in a variety of different configurations, though must use at least two measurement heights of temperature. The accuracy of the estimates of heat flux may be expected to be greater when a larger number of sensors are used, due to the results being less sensitive to the errors in individual measurements. Furthermore, the measurement accuracy in the determination of wind speeds and temperatures also can have a significant influence on the predictions of the method. The accuracy of typical measurements of temperature and wind speed were discussed in Section 2.

Monte Carlo techniques enable the propagation of errors through sets of equations by randomly resampling input data that have been assigned probability distributions. In order to assess the errors that would be likely to occur when using flux-gradient techniques to interpret vertical profiles of wind speed and temperature, Monte Carlo methods were used to propagate errors in these scalars through a set of flux-gradient equations.

Four scenarios were used to assess errors due to sensor configuration and measurement uncertainty. The sensor configurations that were investigated represented the use of measurements at two heights (2 m and 10 m), as often used for providing data for atmospheric dispersion models; and also a more detailed four heights configuration (0.5 m, 0.75 m, 1.0 m & 2.0 m), as often used when conducting micrometeorological research.

The precision of the measurements of temperature and wind speed were defined as inputs to the Monte Carlo model using normal distributions with the mean set to the deterministic value and the range defined by the following error terms (expressed as the 95% confidence limits).

- Temperature: coarse +/- 0.1°C; fine +/- 0.02°C
- Wind speed: coarse +/- 5%; fine +/- 2%

Overall the four sensor precision and configuration scenarios that were used were:

- Scenario 1: Fine sensor precision, measurements made at 2 heights
- Scenario 2: Coarse sensor precision, measurements made at 2 heights
- Scenario 3: Fine sensor precision, measurements made at 4 heights
- Scenario 4: Coarse sensor precision, measurements made at 4 heights

As previously stated, the uncertainty in the estimation of heat fluxes and friction velocities using the flux gradient method was likely to vary with the prevailing meteorological conditions. Hence, wind speeds and temperatures at the above heights were reconstructed from values of $F_{\theta 0}$, u_* and θ_* for seven meteorological scenarios following the Pasquill stability classification system (A-G). These were determined from the Ringway meteorological dataset by processing the data through the meteorological pre-processor of ADMS 3.1 and banding the results into stability classes using the relationship between Monin Obukhov length and stability class derived by Golder (1972). The results of this analysis are shown in Table 2. The values of $F_{\theta 0}$ and u_* that were derived for each stability class, shown in Table 2, were determined as the arithmetic averages of the hourly results. Appendix A details the methods used to reconstruct temperatures and wind speeds from these data.

The Monte Carlo model was run with 5000 different sets of randomly sampled input data (temperatures and wind speeds) for each of the above scenarios. The results are shown in Table 3. Overall Table 3 shows that the flux gradient method provided reasonably consistent estimates of $F_{\theta 0}$ and u_* when comparing the different sensor precision and configuration scenarios. However, during strongly stable conditions (category G) the median friction velocities and heat fluxes output using the 2 point profiles were significantly different from the expected values from Table 2 or the more detailed 4 point profiles. This illustrates that users of the method should be aware that during strongly stable conditions the flux-gradient method can produce spurious results if insufficient data are available to resolve the variations in temperature and wind speed with height.

Table 3 also shows that friction velocities had narrower uncertainty bounds, as shown by the percentile ranges and the coefficients of variation, than the sensible heat fluxes. Sensible heat fluxes were mostly predicted to within 20 – 30% using the coarse precision instrumentation and to within 10% when fine precision instrumentation were simulated. The two stability classes where wider ranges were observed were categories D and G. The large range for category D reflects the very small values of heat flux, a good approximation of the limit of detection of the method, and the fact that fluxes could be either positive or negative in value. The range for category G, for the 4 point profiles, is likely to be due to the dominance of the stability correction terms for this class.

It should be noted that the above analysis only considered the error in estimating fluxes due to measurement uncertainty and did not consider other error terms that may be significant in a real-world situation. These errors may arise from sensor drift, from violations of the implicit assumptions of the method (such as the constant flux layer assumption), and from stochastic variability caused by turbulence in the atmosphere. An estimate of the overall errors in the determination of heat fluxes using on-site micrometeorological methods was made by Hill et al (2002). They compared eddy-correlation and flux-gradient measurements from a site close to the BNFL Sellafield complex. Overall, the coefficient of variation (CV), which is defined as the standard deviation divided by the mean, for the hourly sensible heat flux had a typical value of 0.4 (40%), much higher than observed in Table 3. This indicates that in a realistic situation measurement error may be only one of the contributors to the uncertainty in estimating boundary layer parameters.

An assessment was also made of the likely effect that the measurement errors in heat fluxes and friction velocities could have on the determination of air concentrations using the ADMS 3.1 dispersion model. The assessment was conducted for a 40 m high stack and evaluated air concentrations at 6 downwind distances. A set of 5000 probabilistic meteorological input data were run through the model, generated from the data discussed in the previous section. In order to reduce the duplication of data only data for the 4 point profiles are presented. The data for coarse precision instruments and fine precision instruments are shown in Tables 4 & 5 respectively.

The results in Table 4 show that the uncertainty in the model (expressed as the ratio of the 95th percentile to the 5th percentile) was relatively low for stability classes A-E at distances beyond 700 m downwind, ranging between 1.49 and 1.28. Uncertainties were higher at receptor positions close to the source for all stability classes except A. For category A the uncertainty in air concentrations was relatively constant with distance from the source. This was likely to be due to the plume being well mixed in the vertical in such convective conditions. Uncertainties were much larger for plumes released in Category F and G. This was likely to be due to the extreme sensitivity of ground level air concentrations on the vertical spread of the poorly mixed elevated plume.

The uncertainties in the predictions of the dispersion model, beyond 100 m, were much smaller when the measurement errors in the fine precision instrumentation were considered, being less than 1.10 (or 10%) for categories A-D beyond 100 m, as shown in Table 5. As found in Table 4, uncertainties were higher close to the stack, especially for stability categories D, E and F and for category G the plume was predicted to remain almost completely insulated from the surface. At distances of 700 m and beyond, the highest air concentrations (as the 50th percentile) were associated with stability class E. The model predictions at 700 m downwind for class E also showed a relatively large uncertainty. The combination of high air concentrations and large uncertainty illustrates that particular care should be exercised when interpreting model predictions determined during such conditions.

5.3 Numerical weather prediction datasets

The use of on site meteorological measurements or representative observations from a remote location within dispersion models have been described in earlier sections. Output from a dynamic 3-D weather prediction model provides a further data source. Mirza et al (2002) reviewed the potential use of numerical weather prediction (NWP) datasets as input to dispersion models within their study completed for ADMLC. The Met Office continue to develop their Unified Model (UM) to predict global and regional (mesoscale) movement of weather systems in order to provide weather forecasts for a large range of customers. The mesoscale model assimilates observed data from around the UK, and includes the treatment of a number of important boundary layer processes. It has a horizontal grid resolution of 11 km and vertical resolution of 38 levels, with finer boundary layer resolution than the global configuration. Boundary layer parameters and vertical profiles of speed and temperature are derived within this NWP process.

Topographic forcing within the mesoscale model is limited by the grid scale, so that effects of topographic features on local surface flow may not be reproduced accurately. The NWP model was designed for forecasting over a much larger area than that typically considered within dispersion models and as such cannot be expected to exactly reproduce flow fields over local scale topography. It does, however, provide a representative picture of the average state of the atmosphere over the 11 km grid, rather than providing point specific data such as that from surface measurements.

At present, it is understood that the wind field, temperature, humidity, precipitation, cloud cover (at three heights), boundary layer height and surface heat flux are routinely extracted from the archive. These are processed to deliver an ADMS dataset including a total cloud cover value calculated using randomising overlap algorithms. The surface heat flux and boundary layer height are currently not provided to the customer. Other surface and boundary layer parameters and vertical profiles of wind and temperature are also output from the NWP process, however they are not routinely extracted from the archive. These include friction velocity, Monin Obukhov length, various roughness length scales and soil moisture values. The practicalities, time and expense of extracting all the desired parameters and profiles for dispersion modelling from the NWP archive systems would need to be determined by the Met Office themselves. If available, this data could be directly input to models such as ADMS and AERMOD potentially negating the requirement of the met pre-processors. It should be noted that this system would not be without problems of its own. Continual development of the NWP process by the Met Office will result in increasingly higher resolution of the grid, which may lead to difficulties in processing datasets from different grids to obtain the 5 years sequential data deemed sufficient for assessments by the Environment Agency in their guidance.

5.3.1 Comparison of NWP data and coastal site measurements and their impact on ADMS predictions

In order to promote further discussion on the validity and use of NWP data within dispersion models, Kidd (2002) compared meteorological measurements obtained at Sellafield, a West Cumbria coastal industrial site situated within the influence of Lake District fells to the East, with NWP data for the nearest grid location. The influence of these datasets on ADMS model predictions was then assessed. This study undertaken at Westlakes Research Institute identified that NWP data and site measurements of temperature, wind speed and precipitation displayed good agreement, both hour by hour and in distribution, with the observed data displaying more extreme conditions, eg, high wind speeds and precipitation events.

Figure 2 displays the windroses for the measured dataset, the dataset of the nearest NWP grid to the Sellafield site and Ringway data for 2000. Encouragingly, it can be seen in this instance that the NWP and site measured wind fields show fairly close agreement. The measured wind field displayed more variability in direction than that predicted by NWP, and the NWP did not reproduce the strong westerly conditions measured on site, thought to be due to the local coast influence, however the general trends are reproduced. Due to Sellafield's relatively remote location, Ringway, near Manchester, approximately 150 km from Sellafield is one of the closest Met Office sites from which data is available for use as dispersion model input. It is immediately apparent that the Ringway dataset does not represent local conditions around Sellafield as well as the NWP predictions. This is likely to be due to the large distance between sites and the influence of complex terrain and coastlines at the Sellafield site.

The choice of methods used to calculate boundary parameters (eg, using profile measurements to calculate values externally or inputting solar radiation or cloud cover and allowing ADMS to calculate values) led to significantly different estimates of boundary layer parameters.

Figure 3 displays the frequency of banded values of $F_{\theta 0}$ for a range of inputs. Comparisons of heat flux values estimated within the ADMS pre-processor using a variety of data sources (Ringway cloud cover, NWP cloud cover from two nearest sites, A and B, and site measured solar radiation data) show strong agreement between each other, particularly when compared to estimates calculated using the micro-meteorological flux profile method. Heat fluxes estimated by ADMS using site solar radiation measurements display an increased frequency in the -50 to -100 W/m^2 band (extremely stable conditions). This is thought to be associated with the limitations of using the solar radiation parameter during night time conditions, where the default value of 5 oktas cloud is assumed in the absence of cloud cover records.

The flux profile method calculates boundary layer parameters (eg, $F_{\theta 0}$ and L_{MO}) externally to ADMS. These can then be input to the ADMS pre-processor in a variety of configurations, to obtain estimates of further parameters such as boundary layer height, h . Sensible heat flux using direct estimates from the flux profile method results in more slightly stable conditions (negative $F_{\theta 0}$) than

slightly unstable, with the opposite effect predicted using L_{MO} as ADMS input to calculate sensible heat flux. Both the flux profile methods exhibit a significant increase in frequency of extreme unstable conditions. These results are consistent with boundary layer height estimates (Figure 4), where both flux profile input configurations ($F_{\theta 0}$ and L_{MO}) display a greater frequency of large h , associated with unstable conditions.

The effect on the overall predicted concentrations is more subtle, with the location of annual concentrations highly dependent upon the wind field (ie, independent of the met pre-processor but dependent upon the source of data). Short term concentrations and the magnitude of the annual concentration are highly influenced by wind speed and stability conditions, hence a mixture of effects from source data (wind speed) and processing of data (stability conditions) are combined.

5.4 Summary

Met Office sites providing sufficient (5 years hourly sequential) meteorological data for use in dispersion models are not able to fully represent locations over the whole of the UK. In particular coastal and mountainous areas are poorly represented and industrial sites at these locations, such as Sellafield, must resort to using remote data from a distant Met Office site (potentially non-representative), site observations (sensitive to choice of measurements and method used to estimate boundary layer parameters) or NWP data (complete UK coverage but unable to resolve small scale local topography effects).

Use of high precision instrumentation for the flux-gradient method should result in estimates of boundary layer parameters that would be comparable to the quality of data produced by sonic anemometers. Methodological problems can, however, limit the usefulness of flux-gradient relationships during periods of strong stability, particularly if the resolution of the vertical gradients (number of sensors) is low. The use of sonic anemometry for commercial purposes remains severely limited, however, we consider careful deployment and maintenance of equipment by competent personnel can provide data of a suitable quality for use in dispersion model assessments. NWP datasets appear to provide a promising alternative to the current situation of searching for the most 'representative' data available. Uncertainty attached to these datasets may actually reduce the overall uncertainty of the dispersion modelling process, if the NWP model output is considered to more closely represent real and model domain average boundary layer conditions than those output from the dispersion model meteorological pre-processors using spot measurements from one location.

Measurement error is likely to be often only a minor source of uncertainty as differences between processing methods and the likely violations of assumptions of stationarity, upwind homogeneity and a constant flux layer have been shown from field experiments at the Sellafield site to have more significant influences on model predictions.

Site measurements are likely to appeal to the emergency assessor who may need only to input a single accurate and immediate value of the current wind field and stability in order to fulfil his requirements. The option of obtaining hourly sequential NWP data is likely to be more appealing to the standard industry operator, who may regard the installation of a met station as excessive. Providing it is acceptable to the regulator, the operator is likely to consider the use of NWP in a similar manner to that of measured datasets, where the purchase of met data from either the Met Office or a WMO data supplier is routine for completing modelling assessments. The price of NWP data at present is similar to that of measured data, however, the effect on prices is unknown if further parameters are requested from the archive.

6 ADMS AND AERMOD DISPARITIES DUE TO TREATMENT OF METEOROLOGICAL INPUTS

This section reviews an inter-comparison between ADMS and AERMOD pre-processors and investigates the sensitivity of predicted concentrations upon pre-processor outputs. It also highlights differences associated with user input of roughness length, z_0 , and energy budget parameters (Albedo, r , modified Priestley Taylor parameter used in ADMS, α , and the Bowen Ratio used in AERMOD, β). Differences in annual and short term peak concentrations are examined and where disparities are apparent, the causes are identified.

6.1 Methods

Meteorological data from Ringway was used as input to the ADMS and AERMET pre-processors for the single calendar year of 2000. The data that were supplied to the model were Julian day, time of day, near surface air temperature, wind speed, wind direction, precipitation, cloud cover and relative humidity. In addition to this dataset, further parameter inputs are required by both models.

ADMS defaults to using single values of albedo, r , and modified Priestley Taylor parameter, α , throughout the year, although hourly values can be input through the met file. Most users input surface roughness, z_0 as a single value for the emission site, although it is possible to input values for the met site and/or create a surface roughness grid for the model domain. It is not possible to change surface roughness on a seasonal basis.

The AERMET user selects a suitable site surface characteristic on a sector based level, which automatically assigns default seasonal values of albedo, r , Bowen ratio, β and surface roughness, z_0 . For this modelling study, cultivated grassland (average moisture) was chosen as the surface characteristic. Associated values of r , β and z_0 are given in Table 6. CERC (2001) provide a temperature dependent values of γ/s (see equation 1) that allow simple transfer between the ADMS α parameter and the value of β used in AERMET. Hence it is possible to

set up ADMS and AERMET model configurations with equivalent surface moisture budget parameters (see ADMSseas and AMETseas below) assuming a constant γ/s value for 15°C.

Four meteorological inputs were created for further model testing, two from each pre-processor. The first (labelled def in details below) were created using single values of r , β and z_0 , the second (labelled seas in details below) used seasonal values of r , β in both models and seasonal values of z_0 in AERMET. The following configurations of meteorological, surface energy budget and roughness length inputs were tested:

ADMSdef Output from the ADMS pre-processor using default conditions of r and α . $z_0=0.1$. This dataset represents a standard ADMS user input. Configuration tested on AERMET and the ADMS pre-processor.

ADMSseas Output from the ADMS pre-processor using seasonal values of r and α (Table 6) for average moisture cultivated grassland. z_0 remained at 0.1 m. Configuration tested on AERMET and the ADMS pre-processor.

AMETseas Output from the AERMET pre-processor using default conditions, ie, seasonal values of r , β and z_0 for average moisture cultivated grassland. This configuration is considered typical of a standard AERMOD user. Configuration tested on AERMET and the ADMS pre-processor.

AMETdef Output from the AERMET pre-processor was forced to use ADMS default values of r and equivalent β (Table 6). Configuration tested on AERMET and the ADMS pre-processor.

Estimated parameters such as boundary layer height, sensible heat flux, Monin-Obukhov length and friction velocity output from both models for each of these datasets were compared using graphs to display correlation and statistical analysis tables. The mean bias was used to illustrate the ensemble mean under or over estimation of friction velocity and boundary layer height from one dataset compared to another, given by the ratio of the ensemble mean of the model predictions over the ensemble mean of the measurements. The average difference between hourly values and the associated standard deviation are reported for all parameters, as is the correlation coefficient squared, R^2 . The statistical factors F1.25 and F2 were used to represent the percentage of data from one dataset within a factor of 1.25 of 2 of the values from the dataset with which it was compared. Where parameter values can be negative (heat flux and Monin-Obukhov length) the F factors were calculated for conditions where both data points had positive values and where both data points had negative values. All other hours were excluded from the statistics and reported as the fraction excluded.

Following analysis of the pre-processors outputs, the four datasets were tested against a generic model scenario in both ADMS and AERMOD in order to determine the impact of each dataset on annual average and short term percentile concentrations. In order to incorporate AERMET output into ADMS, friction velocity (u^*) replaced 10 m wind speed input, and boundary layer height,

heat flux and the reciprocal of Monin Obukhov length were added to the standard input parameters. To incorporate AERMETseas, seasonal values of albedo and equivalent Priestley Taylor parameter were used in the input file, however, a single value of 0.3 m was used for roughness length throughout the year.

A non-buoyant emission of SO₂ from a 40 m stack was created as a standard scenario with input parameters and output details provided in Table 7. The following model configurations were also created to test the sensitivity of predictions to urban emission site conditions, to buoyant releases, and to the inclusion (within AERMET) of low wind speed conditions:

Urban: Model configuration run through ADMS using ADMSdef input with z_0 increased to 1 m. Model configuration run through AERMOD using AMETseas input with urban values of r , β and z_0 in AERMET.

40m_b: Model configuration run through ADMS using ADMSdef input and AERMOD using AMETseas input. Exit temperature increased to 130°C and exit velocity increased to 25 m/s.

u0.75: Model configuration run through AERMOD using AMETseas input with minimum wind speed set to 0.75 m/s.

In order to identify disparities for individual hourly conditions, the pre-processor estimates of boundary layer parameters were compared on an hour by hour level using specific days chosen to represent a wide range of conditions throughout the year. Predicted concentrations for periods during these days were also obtained and compared to attempt to identify whether particular disparities in boundary layer parameters strongly influenced model predictions of location and magnitude of maximum concentrations.

6.2 Results

6.2.1 Correlation between yearly distributions of boundary layer parameters

Figure 5 displays the correlation of boundary layer parameters for the ADMSdef and the AMETseas datasets. These were chosen for display as they are the most likely datasets created from processing standard user input to each of the models. Tables 8 to 11 display the statistical analysis of differences in boundary layer parameters.

6.2.1.1 *Boundary Layer Height*

Although there is reasonable correlation between ADMSdef and AMETseas (Table 8), AERMET (using the UA estimation tool rather than upper air data) estimates higher boundary layers than both ADMS and those that might be typical for convective conditions in the UK. This reflects previous findings of Thé et al (2001), who identified that the UA Estimation Tool, written by Lakes Environmental to allow AERMET to process data without upper air soundings,

generally predicted higher boundary layers than those using upper air data. The influence of seasonal energy balance and roughness parameters did not significantly effect the agreement between the model met processor outputs, however AMET boundary layer heights displayed a larger sensitivity than ADMS (assumed to be due to changing values of roughness length). There is a large amount of scatter apparent in figure 5 indicating numerous hours where ADMS estimates boundary layer heights around or below 500 m while AERMET values range up to 3000 m. Figure 6 reveals the hourly and seasonal dependence associated with these large differences between AERMET and ADMS, showing the majority of these occasions occur during the hours of dusk.

Further seasonal analysis (Figure 7) highlights the tendency for ADMS values to be larger than those of AERMET during the winter months when boundary layers are low. This will be due in part to the lower limit of 50 m applied to ADMS values, while the lowest value in AMETseas is 4 m. Stable and complex stratified flows are associated with these low boundary layers and the ability of either model to predict accurate dispersion calculations is limited.

6.2.1.2 Friction velocity

Correlation of friction velocity between all datasets is strong (see Table 9). It is apparent that the friction velocity algorithms are dependent upon surface roughness, hence the appearance of 4 lines of strong correlation in Figure 5 where AMETseas is using seasonal values of z_0 , while ADMSdef uses a constant value of 0.1 m.

6.2.1.3 Sensible Heat Flux

There is strong correlation between heat flux estimates from both the AERMET and ADMS pre-processor (Table 10). Similar differences between the datasets were observed for heat flux as were observed for boundary layer depth and friction velocity. The impact of inputting single or seasonal values of z_0 , r , α or β has the smallest effect on AERMET's estimates of positive heat flux and ADMS's estimates of negative heat flux. AERMET displays a lower limit of -65 W/m^2 (apparent in Figure 5), while ADMS values reach -100 W/m^2 . Although absolute differences over the dusk period did increase slightly (towards 40 W/m^2) during the summer months, this might be expected as fluxes are generally higher during these daylight periods. No daily or seasonal trends in relative differences between the datasets were identified.

6.2.1.4 Convective velocity scale (w_)*

In the instances where both models estimated a convective velocity, values were in fairly good agreement with AERMET predicting larger and much more frequent values than ADMS (see Figure 5). These results again point to AERMET estimating more frequent and extreme convective activity than ADMS.

6.2.1.5 *Monin-Obukhov length*

Correlation between datasets (Table 11) is similar to those of boundary layer heights and poorer than that of heat flux and friction velocity, reflecting the dependence of algorithms on previously calculated parameters. The high F2 factors (0.71 & 0.98) for agreement of AERMET estimates of L_{MO} when using single or seasonal values of z_0 , r , α or β , and similarly high values for ADMS (0.96 & 0.82) suggest a small influence of these parameters on the met pre-processor algorithms for L_{MO} . However, the low F1.25 values for AERMET (0.06 & 0.11) demonstrate that the agreement is not perfect.

Estimates of $1/L_{MO}$ at the minimum limit value of -1.0 /m occur frequently in the AMETseas dataset (Figure 5), never reaching values above 0.7 /m. In contrast, ADMS frequently estimated $1/L_{MO}$ at the maximum limit value of 1.0 /m, with values reaching below -1.5 /m. AERMET generally predicts more strongly unstable conditions than ADMS, while ADMS predicts slightly stronger stability than AERMET (higher positive values of $1/L_{MO}$). The disparate occasions where ADMS predicts low negative values (slightly unstable conditions) and AERMET predicts high positive values (strongly stable conditions) occur where input wind speeds are 0.5 m/s, ie, hours which are not included in ADMS dispersion predictions. There are also occasions where ADMS predicts high strongly stable conditions and AERMET predicts negative values. These frequently corresponded to dusk and dawn hours throughout the year.

Overall agreement between the meteorological pre-processors is relatively encouraging, although conditions are identified where differences are at their greatest. This reflects the subtleties involved in the application of similar meteorological pre-processor methodologies. Similarly, Hall et al (2000) found that although h and L_{MO} values from ADMS and AERMOD calculated from identical input data showed large differences, values of the dimensionless h/L_{MO} showed broader agreement. The smallest differences were found between ADMS pre-processor output using single default values of z_0 , r and α as input compared with using seasonal values of r and α . This suggests the influence of changing z_0 , maybe the largest contributor to differences in processor output from meteorological related input. The impact of these differences on model predictions are investigated in the following sections.

6.2.2 **Comparison of annual average model concentration predictions**

Outputs of both the ADMS and AERMET pre-processors were used as input to both ADMS and AERMOD dispersion models. Predictions of the magnitude and location of the annual average concentration from each model run are given in Table 12. The location of the highest annual average concentration matched to within one grid point for ADMS and AERMOD predictions using default and seasonal values of r , α (or β) and z_0 . Predicted peak concentrations from different meteorological inputs lay within 30% of each other, considered well within the uncertainty range that might typically be associated with a model prediction. Predictions from AERMOD using the AMETseas input ($0.79 \mu\text{g}/\text{m}^3$) and from

ADMS using ADMSdef input ($0.97 \mu\text{g}/\text{m}^3$) were within 23%. These are the predictions that most model users might compare.

ADMS predictions for the 40 m stack height tended to be slightly higher than those from AERMOD. Differences between model predictions for urban conditions did not appear to be significantly greater than those for rural characteristics for this chosen scenario. Differences between the models increased for the buoyant 40 m release scenario, with ADMS predicting an annual average 1.89 times higher than AERMOD. The inclusion or exclusion of wind speeds $<0.75 \text{ m/s}$ did not appear to significantly affect annual averages. Differences in model predictions from using different meteorological input are small compared to changing other input data, such as creating buoyant plumes.

6.2.3 Comparison of peak short term model concentration predictions

Predictions of the peak (100th percentile) concentration and location from each model run are given in Table 13. The location of the peak concentration is not expected to match between model configurations due to peak values being obtained from specific hours. AERMOD peak concentrations displayed greater variability than those of ADMS. ADMS predictions from its pre-processor inputs, using default or seasonal values of r and α , do not appear to vary greatly. However input of AERMET processed data with seasonal variation in r , β and z_0 significantly reduces predictions. This points to differences in values of z_0 influencing pre-processor outputs and subsequently model predictions more strongly than energy budget parameters.

Differences between the predictions from using the most standard datasets in both models is large, with ADMSdef peak value at $82.6 \mu\text{g}/\text{m}^3$ and AMETseas peak at $207.2 \mu\text{g}/\text{m}^3$. Similar trends are seen with the Urban scenario. With the exclusion of hours where wind speeds are less than 0.75 m/s (ie, $u0.75$), peak concentrations in AERMOD are significantly reduced to almost half the previous value (from 207.2 to $112.7 \mu\text{g}/\text{m}^3$), highlighting the fact that peak concentrations are predicted to occur in lowest wind speed conditions, which are modelled in AMETseas but not in $u0.75$ configurations.

It is possible to draw out the six hours resulting in the highest concentrations from the AERMOD .apo output file for comparison with equivalent ADMS values (from the .max file). Table 14 displays the sixth highest hourly concentrations predicted by AERMOD and ADMS using ADMSdef, ADMSseas, AMETseas and AMET_u0.75 model configurations. Very minor changes in peak or sixth highest concentrations are seen with the ADMS results when using default or seasonal values of r and α . Much larger changes are seen between the peak and sixth values for both the AERMOD datasets. The AERMOD results also highlight the large difference in peak short term values when using different lower limits of wind speed. Both the peak and the sixth highest predictions from ADMS and AERMOD predictions match much more closely when lower wind speed limits are in agreement.

6.2.4 Comparison of model predictions from representative days

Figure 8 displays the generally good agreement between ADMS (ADMSdef) and AERMOD (AERMETseas) predictions of peak concentrations over 74 hours on 13 representative days where the large majority of predictions fall well within a factor of 2. The days chosen include:

- neutral conditions - overcast, windy
- stable conditions - clear skies, light winds
- unstable conditions - clear skies, light winds, and
- overcast conditions - light winds.

Figure 9 displays the agreement of downwind distance corresponding with these peak concentrations. Again, the majority of values are well within a factor of two, although ADMS displays more variable distances than AERMOD for the hours displayed.

Table 15 displays examples of individual hours from representative days where agreement between ADMS and AERMOD predicted concentrations were poor, particularly in light wind conditions. The most extreme differences occurred during the dusk and early evening periods of 18:00 March 30th and 16:00 October 21st. On both occasions ADMS predicts a boundary layer limit height of 50 m and slightly stable conditions while AERMOD predicts a higher boundary layer with low but positive sensible heat flux. Boundary layer heights estimated by the pre-processors for October 21st are displayed in Figure 10. This graph highlights the delayed collapse of the boundary layer in AERMET (17:00hrs) compared to that in ADMS (16:00hrs), leading to disparities in predictions for the hour of 18:00hrs. Poor agreement at 13:00hrs December 15th can be traced to ADMS estimating slightly unstable conditions while AERMOD predicts stable conditions.

Table 16 displays examples of individual hours where agreement between ADMS and AERMOD predicted concentrations was good. Moderate or high wind speeds were usually present during these hours, AERMOD often displayed moderate negative heat fluxes with relatively large boundary layer heights. Agreement between both the location and magnitude of the peak hourly concentrations identified remains strong despite large differences between ADMS and AERMOD estimated boundary layer parameters for those hours.

6.3 Summary

As discussed in earlier sections, ADMS and AERMOD follow broadly similar methodologies, however, differences between the systems soon become apparent when attempting to input non-standard met data and when comparing outputs from the two models. Output formats are unsurprisingly different due to the design of the models, with ADMS designed to meet UK regulatory requirements (eg, 99.7th percentiles of peak hourly concentrations) while

AERMOD was originally designed to meet US EPA designs. Hence, a detailed comparison of results entails laborious and costly data processing. However, results from such comparison can provide useful information as this section of the study has shown.

Differences are apparent in the estimated boundary layer parameters from ADMS and AERMOD. Some of these are due to the influence of inputs such as roughness length, while others may be more strongly associated with model parameterisation of the atmosphere and the growth of the PBL throughout the day. These differences are reduced when comparing values of h/L_{MO} which are considered to have a strong influence on dispersion parameters. Conditions of dusk and dawn do show larger disparities between the models, with AERMOD displaying an hour's delay in the influence of the setting sun compared to ADMS. Although peak boundary layer heights are much greater in AERMOD than ADMS, these periods do not appear to create obviously different predictions from the models (apart from dusk hours). Disparities at low wind speeds are also identified. If the model user has identified these conditions as of particular interest, it may be necessary to consider an alternative model with the ability to treat calms and low winds more realistically (ie, CALPUFF (Scire et al, 2000)). The ADMLC has previously investigated dispersion at low wind speed (Lines and Deaves, 1999).

7 PROBABILISTIC MODELLING OF UNCERTAINTY DUE TO METEOROLOGICAL INPUT TO ADMS

This section of the report investigates the impact that uncertainties in meteorological data have on the predictability of both annual average air concentration and the various percentiles of the hourly concentration distributions. Model predictions have been made for SO₂ though it should be noted that no considerations of the deposition or atmospheric chemistry of SO₂ have been made, hence this represents a passive tracer for any chemical or radiological release.

7.1 Methods

The ADMS 3.1 atmospheric dispersion model was chosen for this section of the study as it is often used for predicting the air quality impact of stack emissions within the UK. From a simple consideration of the pre-processing of the meteorological data by ADMS 3.1 (Thomson, 2000) air concentrations would be expected to be relatively unaffected by the changes in relative humidity and air temperature that could occur due to instrument uncertainty or the uncertainty related to the stochastic nature of atmospheric turbulence. Furthermore, as plume depletion due to dry or wet deposition is frequently not considered when assessing compliance with air quality standards, precipitation will not be

considered here. Julian day and time can be accurately determined, however, the treatment of solar elevation by the model, which is a function of day and hour, is an approximation. However, Thomson (2000) suggested that the use of more detailed formulae would not significantly improve the predictability of the model.

From the above consideration it is clear that model predictions of air concentrations are likely to be strongly dependent on the wind speed, wind direction and cloud cover values supplied as input. Further considerations would have to include the roughness length, representing the aerodynamic effects of surface friction, and the assumptions related to the surface energy budget (Priestley-Taylor parameter, α and Albedo, r) as additional sources of uncertainty when processing meteorological data.

Monte Carlo (MC) methods allow the uncertainties in model output to be estimated by carrying out a suitably large number of model runs using random resampling of input data (Hanna et al, 2002). It is necessary, therefore, that appropriate (and realistic) distributions are assigned to the key input parameters. These distributions are themselves subject to a considerable degree of uncertainty, with expert elicitation exercises often being used to estimate the relevant distribution shapes and parameterisations (eg, Pasler-Sauer and Jones, 2000). In order to provide some confidence in the predictions of a Monte Carlo model, Hill et al (2002) compared Monte Carlo predictions with data on the dispersion of stack discharges of ^{41}Ar and ^{85}Kr emitted from BNFL Sellafield. Overall, the model was found to realistically, though not exactly, represent the range of field measurement values.

Monte Carlo methods were applied to ADMS 3.1 by creating 2000 meteorological data files from the original Ringway dataset. Each of these files contained a complete timeseries of hourly Monte Carlo sampled meteorological data for the entire 12 month period. Each meteorological file was assigned to a corresponding ADMS input file (APL file), enabling the modelling of 2000 different realisations of the same meteorological dataset. Meteorological and input (APL) data files were created, and results files were imported into Microsoft Excel™, using code written in Visual Basic Applications Edition (VBAE). All other stack characteristics and receptor details matched those of the 40 m non-buoyant testing scenario detailed earlier in this report. In addition to obtaining the annual average and hourly maximum values for each receptor, the 99.9, 99.8, 99.7, 99.6, 99.5, 99.4, 99.3, 99.2, 99.1, 99, 95, 90 percentiles were also acquired as output.

Three different scenarios were used to evaluate the uncertainty associated with the meteorological data. These were, uncertainties in:

- (i) Basic meteorology (cloud cover, wind speed and wind direction);
- (ii) Basic meteorology and surface energy budget (Priestley-Taylor parameter and Albedo)
- (iii) Basic meteorology, surface energy budget and roughness length.

7.2 Determining appropriate probability distributions

7.2.1 Uncertainty in basic meteorology

The treatment of uncertainty in wind speed and wind direction followed the approach discussed in Hill et al (2002) which presented a simple Monte Carlo model coupled to the R91 atmospheric dispersion code. This model calculated the hourly uncertainty in model input and propagated these through to determine the uncertainty in model calculations of ^{41}Ar external gamma doses and ^{85}Kr air concentrations. The range of model predictions were then compared with a large number of ^{41}Ar and ^{85}Kr field measurements to determine the realism of the modelling approach.

Uncertainties in hourly wind speed, wind direction and σ_0 were determined by Hill et al (2002) by comparing simultaneous measurements of these scalars collected at two meteorological masts, one on each side of the BNFL Sellafield site. Coefficients of variation (standard deviation/mean) were determined for each pair of wind speed and σ_0 measurements and the differences in wind angle between the two meteorological sites were also determined. This analysis of meteorological uncertainty therefore captured both the instrument error and the natural stochastic variation in the meteorological measurements. In order to approximate the variation in meteorological uncertainty with the level of atmospheric turbulence, data were subdivided into nine wind speed bins, with the bounds of each bin being set to ensure that each contained approximately the same number of paired observations (approximately 350).

Uncertainties in the hourly wind speed and wind direction were assumed to follow a normal distribution with a mean given by the original value from the Ringway meteorological datafile. The standard deviation of the wind speed is given by the median coefficient of variation (CV) whilst the standard deviation of the wind direction was approximated by the median wind angle difference. The model used a feedback loop to allow the uncertainties in wind speed and wind direction to vary with the original wind speed, an important finding from the paired meteorological data collected at the BNFL Sellafield site. We have assumed that, in the absence of any other information, the parameterisations of these distributions, and their dependence on wind speed, are broadly applicable across a range of other sites.

The measurements of wind speed and wind direction uncertainty, from Hill et al (2002), are reproduced in Table 17. These results illustrate that uncertainty in wind speeds is inversely proportional to the mean wind speed for wind speeds less than 4.1 m/s, with the highest uncertainty (a CV of 0.19) being found to be associated with mean wind speeds less than 1.9 m/s. Wind speed uncertainty was found to be directly proportional to the mean wind speed for wind speeds higher than the aforementioned threshold, reaching an approximate plateau above 6.0 m/s with a CV of 0.15-0.16. The wind direction uncertainty was found to be inversely proportional to the wind speed, with a peak uncertainty (a median wind angle difference of 31.75°) for wind speeds less than 1.9 m/s. Wind direction uncertainty was found to reach a plateau region above approximately

4.1 m/s with a median wind angle difference of approximately 5.5° (close to the system measurement accuracy quoted in Table 1).

It should be noted that Hill et al (2002) also considered uncertainties in σ_{θ} . However, as σ_{θ} values were not given in the Ringway dataset it was not possible to include this source of uncertainty in the Monte Carlo model.

The uncertainty in the hourly cloud cover was also parameterised using a normal distribution, with the mean given by the original value from Ringway and applying a standard deviation of 1 okta (with no consideration of deteriorating accuracy overnight). The resulting values were rounded to the nearest integer and clipped to ensure that cloud cover could never be less than zero or greater than 8. This would imply a reduction in the uncertainty on cloud cover for periods with an original value of 0 or 8 oktas, though it would be difficult to justify applying a separate model to these data. Furthermore, as identified in an earlier section, the periods when cloud cover of 0 or 8 oktas occur are likely to be under-reported by manual observers using routine methods of cloud observation. It could therefore be argued that the observational data would actually be less uncertain during these periods.

7.2.2 Uncertainty in the surface energy budget

Default parameterisations of the surface energy budget are used by ADMS to calculate heat fluxes and Monin-Obukhov lengths from cloud cover and time of day. ADMS 3.1 uses a Priestley-Taylor parameter (α) of 1 (an estimate of the moisture availability of dry grassland) and a surface albedo value of 0.23. These default values were used for scenario (i). However, it is clear that these parameters are subject to a degree of uncertainty, hence scenarios (ii) and (iii) considered the range that these parameter might take.

In order to estimate the uncertainty on α we have assumed that the values of γ/s contribute a relatively small uncertainty in comparison to that due to assuming a Bowen ratio. The temperature dependence of γ/s was included in the Monte Carlo model as a deterministic value using the data from Holtslag and Van Ulden, (1983) as cited in CERC (2001) and interpolating a value from each hour's surface temperature reading from the Ringway datafile. The uncertainty in the hourly Bowen ratio was included by considering the range of values reported in EPA (1998) for wet and dry grasslands, reproduced in Table 18. A uniform distribution was applied by using the seasonal specific values for wet and dry conditions as the upper and lower limits to the distribution. No account could be made of any diurnal variations in Bowen ratio as ADMS uses Equation 8 to derive sensible heat fluxes with the eddy temperature (θ_*) calculated solely from cloud cover data. A fuller evaluation of the uncertainty in the Priestley-Taylor parameter was beyond the scope of this project.

The surface albedo was also allowed to vary. However, EPA (1998) illustrated that albedo only showed a relatively small variation with season or with land use type. Consequently, the additional complexity for scenarios (ii) and (iii) was limited to considering seasonal deterministic values for surface albedo as

presented in Table 18. These values match the cultivated grassland values given in the AERMET User Guide, which were also used for the ADMS and AERMOD inter-comparisons in the earlier section.

7.2.3 Uncertainty in the roughness length

In scenarios (i) and (ii) a fixed roughness length of 0.1 m was used. This was applied to both the meteorological site and to the source site. For scenario (iii) an estimate of the uncertainty in the roughness length was included in the model simulations.

Uncertainties arise in the roughness length, for most sites, due to the considerable spatial and temporal variability in land use and surface cover. For a dispersing plume the effective roughness length is likely to vary considerably along its trajectory (Hanna and Britter, 2001) whilst few meteorological sites are located in regions where each wind sector will have identical roughness lengths. Furthermore, the upwind "footprint" that elevated measurements correspond with varies strongly with stability (Horst and Wiel, 1994). For example, wind speeds measured at 10 m in stable conditions will be relatively unaffected by nearby short roughness elements, though may be strongly dependent on tall roughness elements several hundred metres upwind.

Hill et al (2002) assumed that the uncertainty in roughness length could be approximated by a log-normal distribution, given that the distribution shape was likely to be strongly skewed by the impossibility of negative or zero values and by the large range that would typically be observed in the field. In this study we considered the roughness length for the meteorological site and for the source site separately, as it is often the case that meteorological sites may be located at a considerable distance from the actual source being considered. The log-normal distribution for the roughness length at the meteorological site was parameterised by assuming that the 5th and 95th percentiles of the distribution were 0.02 m (open grassland) and 0.3 m (agricultural areas) respectively, whilst higher values of 0.1 m (root crops) and 0.5 m (parkland/open suburbia) respectively were applied to the source site.

7.3 Results

Monte Carlo modelling, by its very nature, generates large quantities of data. The 2000 runs that were input per scenario generated more than 1.3 million output data points. In order to simplify this data it is convenient to determine appropriate statistics for describing the range of the results and the median value from the set of simulations. The range of data was evaluated as the ratio of the 97.5th percentile to the 2.5th percentile for the 2000 data points in each simulation for each receptor and output statistic (annual average, etc). This ratio can be interpreted as representing the maximum deviation between values that would be expected at a confidence limit of 95%. The median (the 50th percentile) was determined directly from each data series.

Table 19 shows the ratios of the 97.5th percentile to 2.5th percentile for annual average concentrations of SO₂ at each of the receptor locations and for each of the input data scenarios. Similar ratios were found for scenarios (i) and (ii), varying between 1.06 and 1.33. For these two scenarios the percentile ratios did not vary strongly with distance, though generally higher ratios were found for receptor point locations to the south and west of the source. Results for scenario (iii) showed a substantial increase in percentile ratios over the results presented in the previous scenarios. Furthermore, the results for scenario (iii) showed a substantial reduction in the percentile ranges with distance from the source and their dependence on wind sector was markedly reduced.

The median values from the simulation of annual average SO₂ concentrations are shown in Table 20 alongside the deterministic results from the earlier model runs (as presented in Section 6). MC median values closely match deterministic predictions of annual average using one year's met data as input. All the scenarios returned similar median values at distances of 1000 m and greater, indicating the differences in energy budget and roughness length parameterisations would not significantly bias the model predictions. Furthermore, a good agreement was found between the median values and the deterministic results. Differences between the input scenarios, and between the median probabilistic value and the deterministic calculations were only noticeable at a downwind distance of 250 m from the source. The median concentration values at this distance were found to increase with the complexity of the uncertainty model, such that the highest concentration was predicted for scenario (iii).

The ADMS model was also setup to output various percentiles of the hourly concentration distribution. The uncertainty in these output were also evaluated by looking at the percentile ratios and median values of the Monte Carlo output using the same methods as were applied to the annual average air concentrations.

Table 21 shows the percentile ratios for the ADMS output of the 99.7th percentile of the hourly concentration distribution. The percentile ratios were found to be relatively consistent across scenarios (i), (ii) and (iii) in the Monte Carlo model, with the overall range of values being between 1.09 and 1.41. In general, slightly higher uncertainties were associated with receptor locations to the south and west of the source, though the increase in uncertainty associated with the use of scenario (iii) resulted in this effect being somewhat smoothed out. The percentile ranges reported in Table 21 did not show the strong dependence on downwind distance that was found for the annual average air concentrations.

The median values of the 99.7th percentiles of hourly concentrations predicted by the Monte Carlo model are shown in Table 22, alongside the deterministic values from ADMS. As found with the median values of the annual average air concentration, median 99.7th percentiles of hourly concentrations were relatively unaffected by the use of scenarios (i), (ii) or (iii) in the Monte Carlo model. This illustrates that the application of these scenarios in the Monte Carlo model has not resulted in any significant bias in the model output of the 99.7th percentile of

hourly concentrations. Again, a good agreement was found between the median probabilistic values and the deterministic results, with the largest differences occurring at sites which were shown, in Table 21, to have a wide probabilistic range.

7.4 Summary

The results for the basic meteorological data, scenario (i), provide an indication of the level of irreducible uncertainty in model predictions that would arise from meteorological uncertainties. Overall, the contribution of the uncertainty in basic meteorological data to predictions of both annual average air concentrations and the 99.7th percentile of hourly concentrations was relatively small, with ranges of 1.07–1.33 and 1.09 –1.38 respectively. The higher uncertainties tended to occur at receptors that received relatively infrequent winds from the site and there was a slight increase in uncertainty at the closest receptor location.

Overall, these results showed that the energy budget calculations in ADMS had relatively little impact on the overall uncertainty in annual averaged model outputs, whilst the roughness length contributes a relatively large influence on the model uncertainty that would occur due to the model user's influence on meteorological input data. Consequently, uncertainty can be expected to be relatively large at locations where there are large variations in surface roughness or when using meteorological data collected from a meteorological site located in a relatively heterogeneous landscape.

An interesting finding from this study is that uncertainties associated with the 99.7th percentile of hourly averaged air concentrations are similar (and potentially smaller) than those associated with the annual average concentration. Figure 11 shows the variation in uncertainty of various percentiles of the annual concentration distributions (as defined by the ratios of the 97.5th to 2.5th percentiles of the Monte Carlo output) for two receptor locations, to the north and south of the source at downwind distances of 250 m for scenario (iii). This figure clearly illustrates that the uncertainty in the various percentiles of the hourly concentration distribution tends to reduce before increasing to the 100th percentile (the highest hourly value). The differences between the plots of the receptor to the north and south of the site are likely to result from the large differences in the frequency of wind directions to these receptor sites. A low frequency of winds towards a receptor would result in long periods with a zero (or background) air concentration, with intermittent periods within the plume. Weather conditions and wind direction fluctuations within these periods could vary significantly hence uncertainties in percentile concentrations would increase significantly.

8 GUIDANCE FOR THE MODEL USER COMMUNITY

A significant source of uncertainty in the predictions of atmospheric dispersion models is due to the model formulations and model physics. This applies both to the formulae used to model atmospheric dispersion and the computations of the meteorological pre-processors. The inter-comparison of predictions of the meteorological pre-processors of ADMS and AERMOD, in section 6, has shown that the pre-processors, in general, show larger differences between the modelling systems than due to the uncertainties in parameterising the surface energy budget (ie, α or β , and r). Surface heat flux parameterisations also have an important effect but are not controllable by the user and effects are different between the models. Large differences are also observed between boundary layer parameter estimates from the ADMS pre-processor and from estimates made using the flux profile method to obtain stability data. This project was not designed to recommend the choice of a particular modelling system and broadly follows the recommendation of Carruthers et al (2001) that the differences between the models reflect true uncertainties in estimating turbulent dispersion in the atmospheric boundary layer. The following points summarise the relevant findings of the work completed within the report, however, it should be noted that only one mid-level stack height has been considered within modelling inter-comparisons and the effects of meteorological uncertainty on deposition have not been evaluated.

In order to assess the uncertainty due to model formulations and model physics, users are recommended to conduct an intercomparison of predictions from more than one model. It should be borne in mind that models such as ADMS and AERMOD are based on similar modelling methodologies and often produce broadly similar results. Hence, conducting an intercomparison of results will only be worthwhile when concentrations are close to a benchmark level or when considering a specific period when disparity conditions exist between the models. These disparity conditions, detailed in section 6, include the treatment of dawn and dusk, calm meteorology and the treatment of large and rapid variations in cloud cover. Where frequent calm conditions occur (greater than approximately 10% of the time) and when concentrations are close to a benchmark level, or when modelling a specific period with low wind speeds, model users are recommended to consider the application of a model with a capability to treat such conditions (for example CALPUFF (Scire et al, 2000)). It should be noted that peak air concentrations often are predicted during periods with low wind speed, hence it would be prudent, when reporting the percentiles of a concentration distribution, to reference the frequency of calm conditions, and record the minimum threshold wind speed used within the study.

The choice of meteorological data for input to atmospheric dispersion models also can be of significance. Model users are recommended to assess the representativity of the meteorological site that they use to the conditions at their source location. Previous ADMLC reports have discussed issues of data representativity including distance from observing sites, the use of NWP data and

ageing issues of historic data. Both of the two main UK suppliers of met data for dispersion models provide certificates of representativity upon request, unfortunately they do not routinely state the procedures used to determine the degree of representativity. Modellers intending to use output from one model's meteorological pre-processor as input to another model should consider the representativity of the re-constructed input, in particular the difference in model treatment of roughness length (and associated friction velocity) and surface heat flux.

The use of NWP meteorological data should be considered when the nearest surface observation station may be unrepresentative of the source location. It should be noted however that Met Office NWP data are currently only available with cloud cover output. Ideally, looking towards the future, we might expect higher spatial resolution data tailored to provide the most appropriate input to the dispersion models (ie, providing L_{MO} , u^* and $F_{\theta 0}$ and z_0 directly) to become available. As a further point, the mesoscale model, used to predict weather around the UK, and to provide NWP data for dispersion models, uses more advanced flow dynamics than can be implemented within the current regulatory dispersion models. It is suggested that future developments to the regulatory Gaussian dispersion models could consider how to incorporate the 3-dimensional NWP data.

Site specific wind fields could be modelled by using meteorological measurements recorded by the site operator. For most industries, these records will not extend to the full 5 year period that the Environment Agency requests in order to account for inter-annual variability. The US-EPA recognises this in their guidance and considers one year of site specific data to be acceptable. These on-site data can be relatively easily included when processing meteorological data for AERMOD and ADMS, however model users should be aware of the fetch requirements for obtaining representative meteorological measurements and should ensure that influences of local structures are minimised. The interpretation of locally measured temperature profiles, or sonic anemometer output, to estimate heat fluxes can also be useful, though again a detailed consideration of fetch requirements and instrument precision should be made. It also should be noted that these methods are particularly uncertain during periods of strong atmospheric stability. Measurements of solar radiation at locations close to a site can provide an alternative method of estimating daytime atmospheric stability in ADMS, though the ADMS to AERMOD converter supplied by Lakes Environmental requires cloud cover as input.

A further consideration when using a meteorological data set is to ensure that the met preprocessor has been supplied with accurate data specific to the site that the records were collected. Overall, the meteorological preprocessors were shown to be relatively insensitive to the parameterisation of the surface energy budget, through the choice of Priestley-Taylor parameter, surface albedo or Bowen ratio. Effects that are far more significant were likely to be observed due to uncertainties in the roughness length at the meteorological site. Model users should ensure that they are aware of the appropriate roughness length at the

meteorological site. It may be useful if the Met Office could provide details of the likely variability in roughness lengths at each of their surface observation sites to enable model users to account for this source of uncertainty in their assessments. Furthermore, detailed consideration of an appropriate roughness length for modelling dispersion downwind of a source should be made. For sites where the dispersing plume interacts with a range of scales of roughness elements this could include the consideration of an effective roughness length (eg, Hanna and Britter, 2001), perhaps specified on a sector basis, or the application of a roughness length map (CERC, 2001).

Emergency assessments are often conducted using screening level models that have the advantages of being relatively quick to setup and fast run-times. These models therefore require a lower number of "uncertain" meteorological parameters, though an increase in the uncertainty due to model formulations and model physics is unavoidable. Consideration should be given to the appropriateness of the modelling system used for emergency assessments. Model users should ensure that their system is suitable for the range of meteorological conditions they may encounter. For example, sites where a high annual frequency of calm conditions are observed should consider a modelling system, or methodology, that can operate in these conditions, whilst sites where emergency assessments may be required for tall stacks should ensure that their modelling system can account for vertical variations in turbulence and wind speed. Consideration should also be given, when setting up an emergency assessment system, to the choice of appropriate roughness lengths and the variability in roughness length. When conducting emergency assessments, model users are advised to consider the increased uncertainty, in plume trajectory, spread and the magnitude of peak concentrations during periods of low wind speed, convective conditions, during transition periods (dawn and dusk) and during periods when large and rapid changes in cloud cover occur. These considerations could include applying countermeasures to wider wind sectors or by applying an appropriate safety factor to concentration estimates.

9 RECOMMENDATIONS FOR FURTHER INVESTIGATION

The modelling assessments considered in this report were related to stack discharges, and focussed on a mid-range (40 m) stack height. Further studies could investigate a range of different source types including line and area sources, using similar Monte Carlo probabilistic methods to assess the factors contributing to model uncertainty. A more detailed consideration of the uncertainty in roughness length could also be made including an inter-comparison of the methods used by models to account for spatial variations in Z_0 .

The feasibility of making fuller use of the data supplied by the NWP model in dispersion modelling assessments should be considered. At a simple level this

could include the direct extraction of heat fluxes and friction velocities from the model, thus reducing the errors caused by the re-interpretation of data by model pre-processors. A detailed investigation into the impact of variations in cloud height on energy budget calculations could also be considered. The integration of the 3-dimensional wind field data, supplied by the NWP model, into Gaussian plume models could also be useful. This would be particularly relevant when predictions are required from elevated sources in a strongly stratified boundary layer, or when predictions are required over large downwind distances.

The validation and inter-comparison of meteorological pre-processors predictions with measured vertical gradients in wind speed, wind direction and temperature and with turbulence measurements from sonic anemometers could also help to address the uncertainty found between modelling systems. This may be particularly useful in ensuring that pre-processing algorithms developed overseas are applicable to the climate of the UK.

10 REFERENCES

- Baldocchi DD, Hicks BB and Meyers TP (1988). Measuring biosphere-atmosphere exchange of biologically related gases with micrometeorological methods. *Ecology*, **69**, 1331-1340.
- Barad ML (1958). Project Prairie Grass, A Field Program in Diffusion. *Geophysical Research Papers*, **59**, Vols I and II, AFCRC-TR-58-235, Air Force Cambridge Research Centre, 439 pp.
- Bercowicz R and Prahm LP (1982). Sensible heat-flux estimated from routine meteorological data using the resistance method. *Journal of Applied Meteorology*, **21** (12), 1845-1864.
- Carruthers DJ, Holroyd RJ, Hunt JCR, Weng WS, Robins AG, Apsley DD, Thomson DJ and Smith FB (1994). A new approach to modelling dispersion on the earth's surface. *J Wind Eng Indus Aerodyn*, **52**, 139-153.
- Carruthers DJ and Dyster SJ (2000). Boundary Layer Structure Specifications, ADMS Technical Specification P09/01P/00.
- Carruthers DJ, McHughes CA, Dyster SJ, Robins AG and Thomson DJ (2001). Comments on Model Inter-Comparison Reports. CERC response to Hall et al (2000). http://www.cerc.co.uk/software/pubs/comparison_comments.pdf
- Carruthers DJ, Weng WS, Hunt JCR, Holroyd RJ, McHugh CA and Dyster SJ (2000). Plume/Puff spread and mean concentration module specifications ADMS. Technical Specifications P10/01Q/00 P12/01Q/00.
- CERC (2001). ADMS 3.1 Users Guide. Cambridge Environmental Research Consultants, Cambridge UK.
- Cimorelli AJ, Perry SG, Venkatram A, Weil JC, Paine RJ, Wilson RB, Lee RF, Peters WD (1998). AERMOD, description of model formulation. US Environmental Protection Agency, Research Triangle Park, NC.
- Cimorelli AJ, Perry SG, Venkatram A, Weil JC, Paine RJ, Wilson RB, Lee RF, Peters WD, Brode RW and Pauimer JO (2002). AERMOD: Description of Model Formulation Version 02222, EPA 454/R-02-002d. US Environmental Protection Agency, Research Triangle Park, NC.

- Clarke RH (1979). *A model for short and medium range dispersion of radionuclides released into the atmosphere*. Chilton, NRPB-R91.
- Dyer AJ and Hicks BD (1970). Flux-gradient relationships in the constant flux layer. *Quarterly Journal of the Royal Meteorological Society*, **96**, 715-721.
- Dyer AJ (1981). Flow distortion by supporting structures. *Boundary Layer Meteorology*, **20**, 243-251.
- EPA (1998). Revised draft users guide for the AERMOD meteorological pre-processor AERMET. US Environmental Protection Agency, North Carolina.
- Gifford F A, (1959). Statistical properties of a fluctuation plume dispersion model. *Advances in Geophysics*, **6**, 117-138.
- Golder D (1972). Relations among stability parameters in the surface layer. *Boundary Layer Met*, **3**, 47-58.
- Hall DJ, Spanton AM, Dunkerley F, Bennett M and Griffiths RF (2000). An inter-comparison of the AERMOD, ADMS and ISC dispersion models for regulatory applications. Technical Report P362, Environment Agency.
- Hanna SR and Britter R (2001). The effect of roughness obstacles on flow and dispersion in urban and industrial areas. In: *Proceedings of the seventh international conference on harmonisation within atmospheric dispersion modelling for regulatory purposes*, pp 266-270. European Commission Joint Research Centre Ispra, Italy.
- Hanna SR and Britter RE (2002). Wind Flow and Vapor Cloud Dispersion at Industrial and Urban Sites. Published by CCPS of the AIChE, New York 2002, ISBN 0 8169 0863 X.
- Hanna SR, Wilkinson J, Russell A, Vukovich J, Frey HC (2002). Estimating uncertainties of air quality modelling systems using Monte Carlo approaches. Paper presented to the American Meteorological Society, May 2002.
- Haugen DA, Kaimal JC, Bradley EF (1971). An experimental study of Reynolds stress and heat flux in the atmospheric surface layer. *Quarterly Journal of the Royal Meteorological Society*, **97**, 168-180.
- Hill RA, Lowles I, Teasdale I, Chambers N, Puxley C and Parker T (2001). Comparison between field measurements of ⁸⁵Kr around the BNFL Sellafield reprocessing plant and the predictions of the NRPB-R91 and UK-ADMS atmospheric dispersion models. *Int J Environment and Pollution*, **16** (1-6), 315-327.
- Hill R, Lowles I, Auld V and Parker T (2002). Probabilistic evaluation of models for the atmospheric dispersion of effluents released from a complex site. In: *Proceedings of the eight international conference on harmonisation within atmospheric dispersion modelling for regulatory purposes* (edited by Batchvarova E and Syrakov D), pp 48-52. Bulgarian Academy of Sciences.
- Holtslag AAM and Van Ulden AP (1983). A simple scheme for daytime estimates of the surface fluxes from routine weather data. *J Climate Applied Meteorology*, **22**, 517-529.
- Holtslag AAM and de Bruin HAR (1988). Applied modeling of the nighttime surface energy balance over land. *J Appl Met*, **27**, 689-704.
- Horst TW and Weil JC (1994). How far is far enough? The fetch requirements for micrometeorological measurement of surface fluxes. *Journal of Atmospheric and Oceanic Technology*, **11**, 1018-1025.
- Hunt JCR (1985). Turbulent diffusion from sources in complex flows. *Ann Rev Fluid Mech*, **17**, 447-458.
- Hunt JCR, Holroyd RJ and Carruthers DJ (1988). Preparatory studies for a complex dispersion model. CERC Report HB9/88.
- Hunt JCR, Kaimal JC and Gaynor JE (1988). Eddy structure in the convective boundary layer – new measurements and new concepts. *QJR Meteorol Soc*, **114**, 827-858.

- Kidd J (2002). Comparison of NWP gridded weather data and site specific observed data for use in dispersion models. MSc Thesis for Applied Meteorology, University of Reading.
- LAQM TG03 (2002). Part IV of the Environment Act, 1995. Local Air Quality Management. Technical Guidance TG-03.
- Lines IG and Deaves DM (1999). Atmospheric dispersion at low wind speed. In Atmospheric Dispersion Modelling Liaison Committee Annual Report, 1996–97.
- Lowles I (2002). Model comparison and uncertainty. AQMAU Model uncertainty workshop, June 2002.
- Mirza AK, Nelson N, Weaver KN (2002). An Assessment of Alternative Sources of Met data for Use in Dispersion Modelling. Met Office report produced for ADMLC.
- Moore DJ (1976). Calculation of ground level concentrations for different sampling periods and source locations. *Atmospheric Pollution*, 5160, Amsterdam, Elsevier.
- Nielsen LB, Prahm LP, Bercowicz R et al (1981). Net incoming radiation estimated from hourly global radiation and or cloud observations. *Journal of Climatology*, 1 (3), 255-272.
- Oke TR (1978). *Boundary Layer Climate*. John Wiley and Sons, New York, New York, 372 pp.
- Olesen HR, Brown N (1992). The OML meteorological preprocessor – a software package for the preparation of meteorological data for dispersion models. MST LUFT-A 122. National Environmental Research Institute, DK-4000 Roskilde, Denmark.
- Panofsky HA and Dutton JA (1984). *Atmospheric Turbulence: Models and Methods for Engineering Applications*. John Wiley and Sons, NY, 417 pp.
- Pasler-Sauer J and Jones JA (2000). Probabilistic accident consequence uncertainty analysis of the atmospheric dispersion and deposition module in the COSYMA package. *Radiation Protection Dosimetry*, 90 (3), 331-337.
- Pasquill F and Smith FR (1983). *Atmospheric Diffusion*. John Wiley and Sons Inc, New York, 440 pp.
- Paulson CA (1970). The mathematical representation of wind speed and temperature in the unstable atmospheric surface layer. *Journal of Applied Meteorology*, 9, 857-861.
- Scire JS, Strimaitis DG and Yamartino RJ (2000). A User's Guide for the CALPUFF Dispersion Model (version 5). Earth Tech, Inc, 196 Baker Avenue, Concord, MA 01742 (<http://www.src.com/calpuff/calpuff1.htm>)
- Shi JP, Ng B (2002). Risk based pragmatic approach to address model uncertainty. Paper for the NSCA DMUG meeting, November 2002.
- Smith J (2000). Options for the most appropriate Meteorological data for use in Short Range Dispersion modelling. ADMLC report prepared by the Met Office.
- Sutton MA (1990). The surface-atmosphere exchange of ammonia. PhD thesis, University of Edinburgh.
- Taylor GI (1921). Diffusion by continuous movements. *Proc London Math Soc*, 2 (20), 196-211.
- Thé JL, Thé CL and Johnson MA (2000). User's Guide ISC-AERMOD View, Volume I, Lakes Environmental. ISBN 0-9681806-0-4.
- Thé JL, Lee R and Brode RW (2001). Worldwide Data Quality Effects on PBL Short-Range Regulatory Air Dispersion Models. *Proceedings 7th Int Conf on Harmonisation within Atmospheric Dispersion Modelling for Regulatory Purposes*, Belgirate, Italy, pp 202-206.
- Thom AS (1975). Momentum, mass, and heat exchange of plant communities. In: *Vegetation and the Atmosphere* (edited by Monteith J L), pp 57-109. Academic Press, London.

- Thomson DJ (1992). An analytical solution of Tennekes' equations for the growth of boundary-layer depth. *Boundary Layer Meteorology*, **59**, 227-229.
- Thomson DJ (2000). The met input module, ADMS 3 Technical Specification. Cambridge Environmental Research Consultants. Available from the website URL: <http://www.cerc.co.uk/software/publications.htm>.
- Van Ulden AP and Holtslag AAM (1985). Estimates of atmospheric boundary layer parameters for diffusion applications. *J Climate Appl Meteor*, **24**, 1196-1207.
- Venkatram A (1980). Estimating the Monin-Obukhov length in the stable boundary layer for dispersion calculations. *J Boundary Layer Meteorology*, **19**, 481-485.
- Venkatram A (1992). Vertical dispersion of ground-level releases in the surface boundary layer. *Atmos Environ*, **26A**, 947-949.
- Webb EK (1970). Profile relationships: The log-linear range and extension to strong stability. *Quarterly Journal of the Royal Meteorological Society*, **96**, 67-90.
- Weil JC (1985). Updating applied diffusion models. *J Climate Appl Meteor*, **24** (11), 1111-1130.
- Weil JC, Corio LA and Brower RP (1997). A PDF dispersion model for buoyant plumes in the convective boundary layer. *J Appl Meteor*, **36**, 982-1003.
- WMO (1996). *Guide to meteorological instruments and methods of observation, Sixth Edition*. Publication of the World Meteorological Organisation Publication. ISBN : 92-63-16008-2.
- Zeller K (1993). Eddy diffusivities for sensible heat, ozone and momentum from eddy correlation and gradient measurements. Research Paper RM-131. Fort Collins, US department of agriculture, forest services Rocky Mountain forest and range experiment station.
- Zilitinkevich SS (1972). On the determination of the height of the Ekman boundary layer. *J Boundary Layer Meteorology*, **3**, 141-145.

11 SYMBOLS AND NOTATION

C_p	specific heat capacity of water
Cl	cloud cover (in oktas)
d:	zero plane displacement
$F_{\theta 0}$	sensible heat flux
g	acceleration due to gravity
h	boundary layer depth
h_{ic}	convective boundary layer height
h_{im}	mechanical mixed boundary layer height
k	Von Karman's constant
L_{MO}	Monin Obukhov length
PBL	planetary boundary layer

PG	Pasquill Gifford - stability category
r	surface albedo
RH	relative humidity
Ri	Richardson number
S	rate of change of saturation specific humidity with temperature
T_0	absolute temperature
T_z	temperature at reference height z
T'	turbulent fluctuations in air temperature
T^*	eddy temperature constant
u_z	wind speed at reference height z
u^*	friction velocity
w	vertical wind velocity
w'	turbulent fluctuations in vertical velocity
w^*	convective velocity scale
z	vertical height (m)
z_0	roughness length (m)
α	modified Priestley Taylor parameter
β	Bowen ratio
θ_z	potential temperature at height z ($^{\circ}\text{C}$)
θ^*	eddy potential temperature constant
λ	specific latent heat of vapourisation of water
Φ_z	wind direction at reference height z
ρ_a	density of air
σ_v	lateral turbulence parameter
σ_w	vertical turbulence parameter
σ_y	lateral dispersion parameter
σ_{ya}	ambient atmospheric turbulence component
σ_{yb}	source buoyancy induced turbulence component
σ_{yc}	building downwash induced component

σ_{yt}	lateral turbulence induced component
σ_{yw}	wind direction unsteadiness component
σ_z	vertical dispersion parameter
σ_θ	standard deviation of wind direction
Ψ_H	empirically derived stability correction factors for heat
Ψ_M	empirically derived stability correction factors for momentum

12 TABLES

Table 1: System resolution and accuracy for in-situ digital measurements recommended by the US-EPA

Variable	System Accuracy	Measurement resolution	Sensor specification
Wind speed	$\pm (0.2 \text{ m/s} + 5\% \text{ of observed})$	0.1 m/s	Threshold $\leq 0.5 \text{ m/s}$
Wind direction	$\pm 5 \text{ degrees}$	1 degree	Threshold $\leq 0.5 \text{ m/s} @ 10 \text{ deg}$
Ambient temperature	$\pm 0.5 \text{ }^\circ\text{C}$	0.1 $^\circ\text{C}$	Time constant $\leq 1 \text{ min}$
Vertical temperature difference	$\pm 0.1 \text{ }^\circ\text{C}$	0.02 $^\circ\text{C}$	
Precipitation	$\pm 10\% \text{ of observed or } \pm 5 \text{ mm}$	0.3 mm	
Solar radiation	$\pm 5\% \text{ of observed}$	10 W/m^2	2 nd class standard resolution $> \pm 10 \text{ W/m}^2$ Spectral response 285 nm to 2800 nm
Pressure	$\pm 3 \text{ mb (0.3 kPa)}$	0.5 mb	
Vertical ΔT	$\pm 0.1 \text{ }^\circ\text{C}$	0.02 $^\circ\text{C}$	Time constant $\leq 1 \text{ min}$
Dew point temperature	$\pm 1.5 \text{ }^\circ\text{C}$	0.1 $^\circ\text{C}$	Time constant $\leq 30 \text{ min}$

Table 2: Analysis of the Ringway 2000 meteorological dataset to derive the frequency of occurrence of each of 7 stability classes, F(SC), and the average boundary layer properties for each class

The ADMS 3.1 meteorological pre-processor was used to derive boundary layer parameters from the original dataset and the relationship between Monin-Obukhov length and stability class from Golder (1972) was used for the banding of values, $z_0=0.1$

Stability Class	Frequency of u SC	u^* (m s^{-1})	u^* (m s^{-1})	$F_{\theta 0}$ (W m^{-2})	h (m)	θ^* ($^\circ\text{C}$)	L_{MO} (m)
A	0.03	1.17	0.15	68.99	542	-0.389	-4
B	0.03	2.14	0.22	63.05	630	-0.23126	-15
C	0.08	3.43	0.33	56.18	687	-0.14256	-56
D	0.47	6.14	0.53	-7.1	625	0.011106	1820
E	0.19	3.38	0.25	-19.99	146	0.06475	68
F	0.06	2.29	0.13	-10.3	57	0.066589	19
G	0.13	1.31	0.03	-1.87	50	0.055283	1

Table 3: Error analysis on the effect of measurement error and sensor configuration on the predictions of the flux-profile method for estimating heat fluxes and friction velocities

CV: coefficient of variation (standard deviation/ mean)

Stability class	Number of heights	Coarse				Fine			
		95 %ile	50 % ile	5 %ile	CV	95 %ile	50 % ile	5 %ile	CV
Friction velocity ($m s^{-1}$)									
A	4	0.14	0.15	0.16	0.05	0.15	0.15	0.15	0.02
	2	0.13	0.15	0.17	0.08	0.14	0.15	0.16	0.03
B	4	0.20	0.22	0.24	0.05	0.21	0.22	0.23	0.02
	2	0.19	0.22	0.25	0.08	0.21	0.22	0.23	0.03
C	4	0.30	0.33	0.36	0.06	0.32	0.33	0.34	0.02
	2	0.29	0.33	0.37	0.08	0.31	0.33	0.35	0.03
D	4	0.48	0.53	0.58	0.06	0.51	0.53	0.55	0.03
	2	0.45	0.53	0.61	0.09	0.50	0.53	0.56	0.03
E	4	0.22	0.25	0.28	0.07	0.24	0.25	0.26	0.03
	2	0.22	0.27	0.32	0.11	0.25	0.27	0.29	0.04
F	4	0.11	0.13	0.15	0.11	0.12	0.13	0.14	0.04
	2	0.16	0.19	0.23	0.11	0.18	0.19	0.20	0.04
G	4	0.02	0.04	0.06	0.30	0.03	0.04	0.05	0.11
	2	0.27	0.30	0.35	0.08	0.29	0.30	0.32	0.03
Heat flux ($W m^{-2}$)									
A	4	48.6	68.9	91.1	0.19	64.3	68.5	72.7	0.04
	2	35.5	68.8	111.2	0.33	60.9	68.6	76.8	0.07
B	4	46.2	62.8	81.9	0.17	59.0	62.7	66.3	0.04
	2	35.4	62.6	96.3	0.29	56.7	62.7	69.2	0.06
C	4	38.2	55.8	75.7	0.20	52.0	56.0	59.9	0.04
	2	32.6	55.8	83.5	0.27	50.7	55.8	61.1	0.06
D	4	-27.6	-7.2	14.1	-1.78	-11.3	-7.1	-2.8	-0.37
	2	-24.6	-7.2	11.9	-1.62	-10.7	-7.1	-3.5	-0.31
E	4	-28.2	-20.0	-11.1	-0.26	-22.0	-20.0	-18.2	-0.06
	2	-29.6	-22.6	-16.5	-0.18	-25.3	-23.1	-20.9	-0.06
F	4	-13.2	-10.2	-7.5	-0.17	-11.5	-10.5	-9.6	-0.05
	2	-27.5	-22.0	-16.9	-0.15	-24.3	-22.1	-20.0	-0.06
G	4	-7.8	-3.7	-1.3	-0.51	-5.0	-3.7	-2.5	-0.21
	2	-234.3	-192.6	-155.7	-0.12	-208.7	-192.6	-177.4	-0.05

Table 4: Dispersion factors ($s\ m^{-3}$) at 6 downwind distances from a 40 m stack for the uncertainties in heat fluxes and friction velocities for the 4 point profile for coarse precision instrumentation

NA: divide by zero OR: over-range

Stability Class		100 m	400 m	700 m	1000 m	1500 m	2000 m
A	95%ile	1.06E-04	1.61E-05	6.49E-06	3.90E-06	2.32E-06	1.67E-06
	50%ile	9.49E-05	1.34E-05	5.50E-06	3.33E-06	1.99E-06	1.43E-06
	5%ile	8.32E-05	1.15E-05	4.79E-06	2.92E-06	1.75E-06	1.25E-06
	95:5	1.28	1.40	1.35	1.34	1.33	1.33
	95%ile	3.87E-05	1.78E-05	6.38E-06	3.37E-06	1.75E-06	1.14E-06
B	50%ile	2.54E-05	1.55E-05	5.47E-06	2.91E-06	1.52E-06	9.95E-07
	5%ile	1.49E-05	1.36E-05	4.76E-06	2.55E-06	1.34E-06	8.80E-07
	95:5	2.60	1.31	1.34	1.32	1.30	1.30
	95%ile	2.60E-06	1.68E-05	7.47E-06	3.93E-06	1.86E-06	1.10E-06
	50%ile	1.13E-06	1.52E-05	6.49E-06	3.31E-06	1.55E-06	9.21E-07
C	5%ile	4.38E-07	1.40E-05	5.68E-06	2.85E-06	1.33E-06	7.93E-07
	95:5	5.93	1.20	1.31	1.38	1.40	1.39
	95%ile	4.34E-09	9.12E-06	6.84E-06	4.60E-06	2.67E-06	1.77E-06
	50%ile	2.41E-10	7.98E-06	6.14E-06	4.11E-06	2.37E-06	1.57E-06
	5%ile	7.41E-11	7.14E-06	5.55E-06	3.59E-06	1.97E-06	1.24E-06
D	95:5	58.58	1.28	1.23	1.28	1.35	1.43
	95%ile	2.48E-12	1.10E-05	1.06E-05	7.83E-06	5.22E-06	3.87E-06
	50%ile	8.62E-17	4.36E-06	7.93E-06	6.95E-06	4.82E-06	3.56E-06
	5%ile	1.64E-23	8.93E-07	4.32E-06	5.27E-06	4.34E-06	3.04E-06
	95:5	OR	12.35	2.45	1.49	1.20	1.28
E	95%ile	0.00E+00	2.65E-07	2.94E-06	4.74E-06	5.03E-06	4.39E-06
	50%ile	0.00E+00	1.11E-10	7.99E-08	5.15E-07	1.45E-06	1.99E-06
	5%ile	0.00E+00	3.31E-15	5.24E-10	2.09E-08	2.12E-07	5.32E-07
	95:5	NA	OR	5613.15	227.22	23.69	8.25
	95%ile	0.00E+00	0.00E+00	1.10E-20	1.65E-15	6.95E-12	3.13E-10
F	50%ile	0.00E+00	0.00E+00	0.00E+00	0.00E+00	4.12E-19	1.47E-15
	5%ile	0.00E+00	0.00E+00	0.00E+00	0.00E+00	0.00E+00	0.00E+00
	95:5	NA	NA	NA	NA	NA	NA
G	95:5	NA	NA	NA	NA	NA	NA

Table 5: Dispersion factors ($s\ m^{-3}$) at 6 downwind distances from a 40 m stack for the uncertainties in heat fluxes and friction velocities for the 4 point profile for fine precision instrumentation

NA: divide by zero OR: over-range

Stability Class	100 m	400 m	700 m	1000 m	1500 m	2000 m	
A	95%ile	1.00E-04	1.39E-05	5.68E-06	3.45E-06	2.07E-06	1.49E-06
	50%ile	9.58E-05	1.34E-05	5.50E-06	3.33E-06	1.99E-06	1.43E-06
	5%ile	9.12E-05	1.30E-05	5.34E-06	3.23E-06	1.92E-06	1.37E-06
	95:5	1.10	1.07	1.06	1.07	1.08	1.09
B	95%ile	2.99E-05	1.60E-05	5.64E-06	2.99E-06	1.57E-06	1.03E-06
	50%ile	2.55E-05	1.56E-05	5.47E-06	2.90E-06	1.52E-06	9.95E-07
	5%ile	2.16E-05	1.51E-05	5.31E-06	2.82E-06	1.47E-06	9.62E-07
	95:5	1.39	1.06	1.06	1.06	1.06	1.07
C	95%ile	1.49E-06	1.58E-05	6.69E-06	3.42E-06	1.60E-06	9.51E-07
	50%ile	1.14E-06	1.53E-05	6.49E-06	3.31E-06	1.55E-06	9.18E-07
	5%ile	8.74E-07	1.49E-05	6.32E-06	3.20E-06	1.50E-06	8.88E-07
	95:5	1.71	1.06	1.06	1.07	1.07	1.07
D	95%ile	4.00E-10	8.08E-06	6.42E-06	4.36E-06	2.53E-06	1.68E-06
	50%ile	2.42E-10	7.74E-06	6.16E-06	4.18E-06	2.44E-06	1.62E-06
	5%ile	1.83E-10	7.43E-06	5.90E-06	3.99E-06	2.30E-06	1.51E-06
	95:5	2.18	1.09	1.09	1.09	1.10	1.11
E	95%ile	1.18E-15	5.58E-06	8.62E-06	7.27E-06	5.07E-06	3.75E-06
	50%ile	8.52E-17	4.38E-06	7.96E-06	7.05E-06	4.94E-06	3.59E-06
	5%ile	3.02E-18	3.21E-06	7.18E-06	6.78E-06	4.80E-06	3.44E-06
	95:5	391.55	1.74	1.20	1.07	1.06	1.09
F	95%ile	0.00E+00	1.59E-09	2.80E-07	1.13E-06	2.28E-06	2.69E-06
	50%ile	0.00E+00	1.22E-10	8.40E-08	5.33E-07	1.48E-06	2.03E-06
	5%ile	0.00E+00	4.79E-12	1.83E-08	2.04E-07	8.47E-07	1.39E-06
	95:5	NA	332.37	15.34	5.52	2.69	1.93
G	95%ile	0.00E+00	0.00E+00	0.00E+00	1.60E-21	8.75E-16	4.26E-13
	50%ile	0.00E+00	0.00E+00	0.00E+00	0.00E+00	3.48E-19	1.30E-15
	5%ile	0.00E+00	0.00E+00	0.00E+00	0.00E+00	3.80E-25	4.82E-20
	95:5	NA	NA	NA	NA	OR	OR

Table 6: Seasonal values of energy balance and surface roughness parameters for cultivated land

Source: Thé et al (2001) AERMET user guide

Relationship between Bowen ratio and Priestley Taylor parameter based on an average annual temperature of 15°C

Season	Bowen ratio (ave moisture)	Priestley Taylor parameter	Albedo (ADMS)	Roughness length
Spring	0.3	1.23	0.14	0.03
Summer	0.5	1.07	0.2	0.20
Autumn	0.7	0.94	0.18	0.05
Winter	1.5	0.64	0.6	0.01
<i>ADMS default</i>	<i>0.6</i>	<i>1</i>	<i>0.23</i>	<i>0.1</i>

Table 7: Input parameters for the 40 m model test case scenario

Stack Parameters	Stack Characteristics
Emission height	40 m
Emission diameter	1m
Efflux velocity	5 m/s
Efflux temperature	15°C
Emission substance	SO ₂
Emission rate	1 g/s
Gridding	-1000 to 1000 m, 64.5 m spacing
Receptor locations	250, 500, 1000, 1500 to N, S, E & W
Output concentrations	Annual and hourly average

Table 8: Statistical comparison of AERMET and ADMS boundary layer height

h	AMETseas- AMETdef	ADMSseas- ADMSdef	AMETseas- ADMSseas	AMETseas- ADMSdef
Mean bias (ratio of model/measured)	0.83	0.96	1.48	1.42
Average Difference	-122	-18	197	303
SD of difference	262	90	389	389
R2 Correlation	0.83	0.94	0.57	0.57
F1.25	0.35	0.91	0.32	0.33
F2	0.90	0.96	0.77	0.77

Table 9: Statistical comparison of AERMET and ADMS friction velocity

U^*	AMETseas- AMETdef	ADMSseas- ADMSdef	AMETseas- ADMSseas	AMETseas- ADMSdef
Mean bias (ratio of model/measured)	0.85	0.99	0.88	0.87
Average Difference	-0.052	-0.001	-0.043	-0.045
SD of difference	0.087	0.008	0.091	0.091
R2 Correlation	0.85	1.00	0.84	0.84
F1.25	0.48	0.97	0.48	0.45
F2	0.96	0.97	0.91	0.91

Table 10: Statistical comparison of AERMET and ADMS heat flux

$F_{\theta 0}$	AMETseas- AMETdef	ADMSseas- ADMSdef	AMETseas- ADMSseas	AMETseas- ADMSdef
Average Difference	-0.38	-3.07	8.68	6.94
SD of difference	10.05	9.12	13.84	34.93
R2 Correlation	0.96	0.95	0.87	0.86
$F_{\theta 0}$ positive F1.25	0.58	0.32	0.31	0.29
$F_{\theta 0}$ positive F2	0.95	0.80	0.70	0.73
$F_{\theta 0}$ negative F1.25	0.36	0.92	0.34	0.34
$F_{\theta 0}$ negative F2	0.95	0.97	0.84	0.85
Fraction Excluded	0.03	0.03	0.08	0.08

Table 11: Statistical comparison of AERMET and ADMS Monin-Obukhov length

$1/L_{MO}$	AMETseas- AMETdef	ADMSseas- ADMSdef	AMETseas- ADMSseas	AMETseas- ADMSdef
Average Difference	0.015	0.006	-0.083	-0.094
SD of difference	0.060	0.072	0.238	0.251
R2 Correlation	0.85	0.95	0.55	0.57
$F_{\theta 0}$ positive F1.25	0.06	0.91	0.03	0.03
$F_{\theta 0}$ positive F2	0.71	0.96	0.49	0.50
$F_{\theta 0}$ negative F1.25	0.11	0.39	0.18	0.21
$F_{\theta 0}$ negative F2	0.98	0.82	0.57	0.65
Fraction excluded	0.03	0.03	0.08	0.08

Table 12: Annual average concentrations

Model input	ADMS				AERMOD			
	Stack height	Buoy- ancy	X(m)	Y(m)	Conc ($\mu\text{g}/\text{m}^3$)	X(m)	Y(m)	Conc ($\mu\text{g}/\text{m}^3$)
ADMSdef	40	N	67	400	0.97	67	400	0.95
ADMSseas	40	N	67	400	0.94	67	467	0.90
AMETdef	40	N	67	400	0.99	67	400	1.03
AMETseas	40	N	67	400	1.00	67	400	0.79
URBAN	40	N	0	267	1.61	0	267	1.48
40m_b	40	Y	67	533	0.34	133	600	0.18
u0.75	40	N				67	400	0.78

Table 13: Maximum (100th%) hourly average concentrations

Model Input	ADMS					AERMOD				
	Date	Hour	X(m)	Y(m)	Conc ($\mu\text{g}/\text{m}^3$)	Date	Hour	X(m)	Y(m)	Conc ($\mu\text{g}/\text{m}^3$)
ADMSdef	19/06	06	-133	200	82.6	02/05	06	-400	0	67.6
ADMSseas	19/06	06	-133	200	89.7	06/04	07	-267	67	100.4
AMETdef	19/06	06	-133	200	88.9	13/01	11	133	67	195.3
AMETseas	30/09	13	-67	67	76.7	02/05	07	-133	67	207.2
URBAN	19/06	06	-67	67	62.2	21/07	06	-200	200	88.5
40m_b	30/05	09	0	133	12.2	23/08	10	-267	0	5.0
u0.75						20/02	10	-67	333	112.7

Table 14: Sixth highest hourly concentrations

	ADMS (ADMSdef)	ADMS (ADMSseas)	AERMOD (AMETseas)	AERMOD (AMET_u0.75)
	Conc ($\mu\text{g}/\text{m}^3$)	Conc ($\mu\text{g}/\text{m}^3$)	Conc ($\mu\text{g}/\text{m}^3$)	Conc ($\mu\text{g}/\text{m}^3$)
Highest hour	82.6	89.7	207.2	112.7
Sixth highest hour	51.4	52.9	141.2	34.8

Table 15: Sample hours of poor agreement between ADMS and AERMOD predictions

Date	Hour	Model	u	T	Cl	h	$F_{\theta 0}$	L_{MO}	Distance	Conc ($\mu\text{g}/\text{m}^3$)
Jan 08	06	AERMOD	4.1	4.8	1	189	-21.3	239	1323	0.89
		ADMS				160	-34.4	76	602	5.8
Mar 30	18	AERMOD	2.6	10.0	2	1541	1	-549	537	14.8
		ADMS				50	-14.8	15	5148	0.93
Mar 31	17	AERMOD	1.0	9.1	6	631	18.1	-4	188	28.7
		ADMS				50	-0.56	1	Peak beyond 10 km	
Jun 15	20	AERMOD	2.6	14.8	6	303	-3.8	403	520	16.5
		ADMS				79	-13.6	33	1736	3.1
Oct 21	16	AERMOD	2.1	11.3	4	686	10.9	-44	333	22.2
		ADMS				50	-5.2	3	Peak beyond 10 km	
Dec 15	13	AERMOD	2.1	4.2	5	77	-2.3	43	1323	1.2
		ADMS				216	5.4	-115	427	14.8

Table 16: Sample hours of good agreement between ADMS and AERMOD predictions

Date	Hour	Model	u	T	Cl	h	F _{θ0}	L _{MO}	Distance	Conc (µg/m ³)
Apr 03	16	AERMOD	9.3	2.9	8	1948	9.8	-998	569	6.0
		ADMS				1463	-6.8	0.0001	422	4.6
Jun 21	04	AERMOD	7.2	15.4	8	1421	-39.6	860	507	6.4
		ADMS				572	-27.1	769	508	5.9
Jun 21	20	AERMOD	6.7	15	6	1315	-5.7	5009	426	8.2
		ADMS				524	-30.2	555	521	6.3
Jun 21	21	AERMOD	7.2	13.5	5	1399	-64	517	388	6.6
		ADMS				462	-54.4	370	538	5.9
Jul 21	20	AERMOD	3.6	21.5	5	492	-13.2	298	471	11.3
		ADMS				150	-24.5	77	745	7.4
Jul 21	21	AERMOD	4.1	19.5	5	552	-34.1	151	679	8.3
		ADMS				189	-28.9	106	745	7.4
Oct 22	09	AERMOD	3.1	9.0	5	285	15.4	-89	388	18.8
		ADMS				202	9.8	-196	389	14.8
Oct 25	12	AERMOD	8.2	11.3	7	1137	33.2	-658	400	7.6
		ADMS				1300	16.8	-2000	400	5.8

Table 17: Analysis of the uncertainty in meteorological data determined from paired meteorological measurements

Data reproduced from Hill et al (2002)

Wind Speed bin (m s ⁻¹)	Median coefficient of variation for Wind Speed (non dimensional)	Median Wind Angle Difference (degrees)
<1.9	0.19	31.75
>1.9 <2.5	0.17	22.15
>2.5 < 3.2	0.13	14.62
>3.2 <4.1	0.12	10.04
>4.1 <5.0	0.13	5.93
>5.0 <6.0	0.14	5.32
>6.0 <6.9	0.15	5.35
>6.9 <8.1	0.16	5.52
>8.1	0.15	5.27

Table 18: Variations in Bowen-ratios and surface albedo for grassland

Season	Bowen ratio		Albedo
	Dry surface	Wet surface	
Spring	1.0	0.3	0.18
Summer	2.0	0.4	0.18
Autumn	2.0	0.5	0.20
Winter	2.0	0.5	0.60

Table 19: Range of possible values (expressed at the 95% confidence level) for the annual average concentration of SO₂ determined from 2000 datapoints

	North	East	South	West
Distance = 250 m				
Scenario (i)	1.12	1.16	1.33	1.25
Scenario (ii)	1.10	1.12	1.27	1.20
Scenario (iii)	2.18	1.73	2.05	1.46
Distance = 500 m				
Scenario (i)	1.07	1.10	1.23	1.18
Scenario (ii)	1.06	1.09	1.20	1.16
Scenario (iii)	1.41	1.26	1.50	1.28
Distance = 1000 m				
Scenario (i)	1.07	1.11	1.25	1.17
Scenario (ii)	1.07	1.11	1.23	1.18
Scenario (iii)	1.21	1.15	1.33	1.23
Distance = 1500 m				
Scenario (i)	1.08	1.13	1.27	1.18
Scenario (ii)	1.08	1.13	1.26	1.19
Scenario (iii)	1.22	1.15	1.31	1.22

Table 20: Median annual average concentration of SO₂ determined from 2000 datapoints

	North	East	South	West
Distance = 250 m				
Scenario (i)	0.69	0.60	0.16	0.27
Scenario (ii)	0.81	0.70	0.18	0.32
Scenario (iii)	1.11	0.86	0.23	0.36
Deterministic	0.71	0.64	0.13	0.29
Distance = 500 m				
Scenario (i)	0.85	0.54	0.14	0.20
Scenario (ii)	0.86	0.52	0.13	0.19
Scenario (iii)	0.99	0.57	0.15	0.21
Deterministic	0.90	0.57	0.12	0.21
Distance = 1000 m				
Scenario (i)	0.46	0.26	0.07	0.10
Scenario (ii)	0.45	0.24	0.06	0.09
Scenario (iii)	0.47	0.25	0.07	0.10
Deterministic	0.49	0.27	0.06	0.10
Distance = 1500 m				
Scenario (i)	0.28	0.15	0.04	0.06
Scenario (ii)	0.27	0.14	0.04	0.06
Scenario (iii)	0.28	0.14	0.04	0.06
Deterministic	0.29	0.16	0.04	0.06

Table 21: Range of possible values (expressed at the 95% confidence level) for the 99.7th percentile of hourly concentrations of SO₂ determined from 2000 datapoints

	North	East	South	West
Distance = 250 m				
Scenario (i)	1.19	1.16	1.38	1.22
Scenario (ii)	1.16	1.15	1.24	1.21
Scenario (iii)	1.29	1.25	1.41	1.26
Distance = 500 m				
Scenario (i)	1.16	1.15	1.22	1.24
Scenario (ii)	1.15	1.13	1.20	1.23
Scenario (iii)	1.28	1.24	1.22	1.22
Distance = 1000 m				
Scenario (i)	1.11	1.11	1.19	1.16
Scenario (ii)	1.09	1.11	1.19	1.16
Scenario (iii)	1.13	1.14	1.24	1.19
Distance = 1500 m				
Scenario (i)	1.09	1.12	1.27	1.20
Scenario (ii)	1.09	1.12	1.27	1.21
Scenario (iii)	1.14	1.19	1.35	1.27

Table 22: Median values of the 99.7th percentile of hourly concentrations of SO₂ determined from 2000 datapoints

	North	East	South	West
Distance = 250 m				
Scenario (i)	23.46	23.73	15.40	22.52
Scenario (ii)	22.40	21.59	15.16	20.71
Scenario (iii)	22.98	21.91	16.04	20.71
Deterministic	23.84	23.91	11.68	24.23
Distance = 500 m				
Scenario (i)	12.79	12.38	8.57	11.13
Scenario (ii)	11.90	11.08	7.75	9.89
Scenario (iii)	11.61	10.88	8.01	9.69
Deterministic	13.04	12.13	8.23	10.51
Distance = 1000 m				
Scenario (i)	6.01	5.86	4.43	5.36
Scenario (ii)	5.77	5.54	4.19	5.00
Scenario (iii)	5.83	5.57	4.20	4.97
Deterministic	5.98	5.91	4.28	5.22
Distance = 1500 m				
Scenario (i)	4.13	3.97	2.88	3.56
Scenario (ii)	4.03	3.82	2.75	3.37
Scenario (iii)	4.04	3.82	2.76	3.32
Deterministic	4.16	3.96	2.62	3.67

13 FIGURES

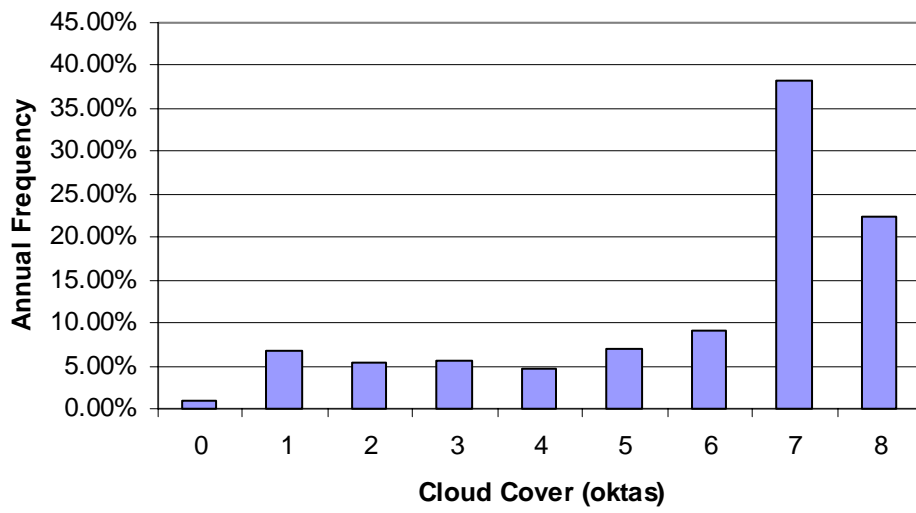
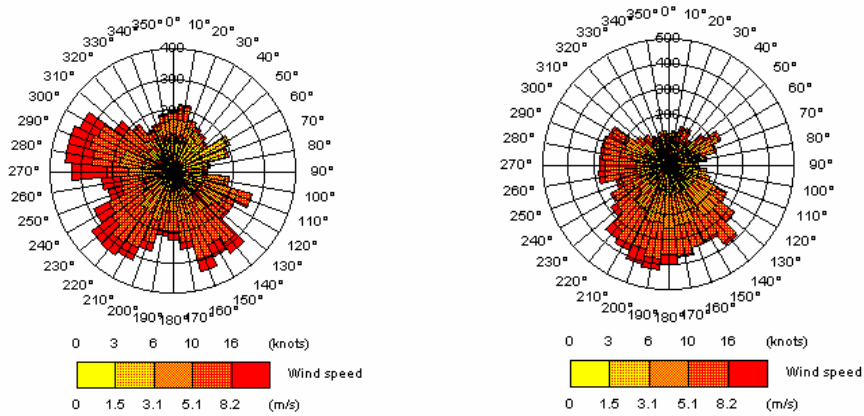
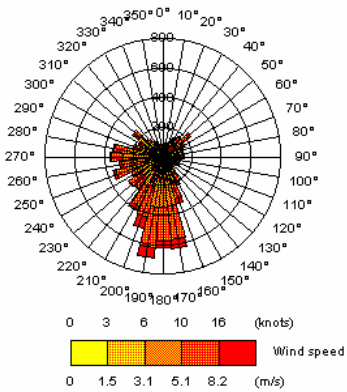


Figure 1: Frequency of cloud cover for Ringway 2000 dataset



a) Sellafield site measurements

b) NWP from nearest grid to Sellafield



c) Ringway Met Office site measurements

Figure 2: Wind roses from a) measurements at Sellafield site, b) nearest NWP grid, and c) Ringway for 2000.¹

¹Wind roses created using ADMS windrose viewer

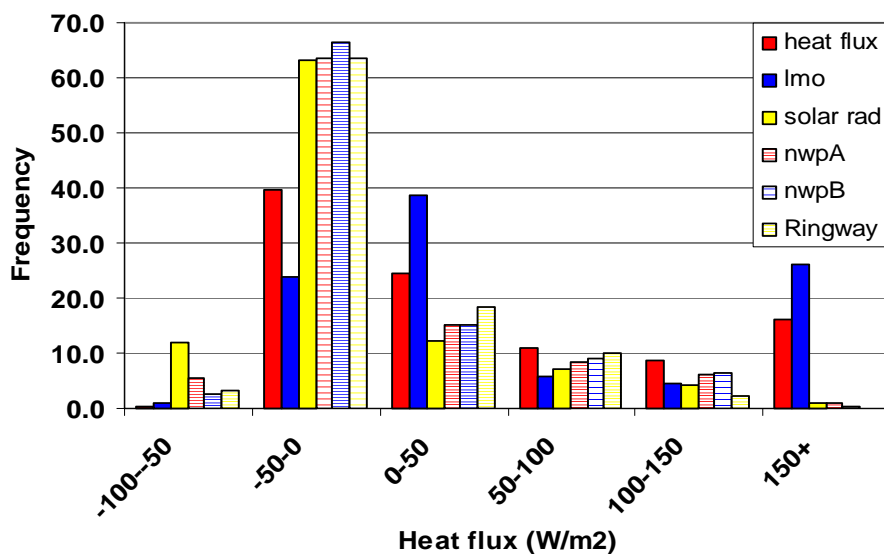


Figure 3: Binned frequency of heat flux estimates from 5 different met data inputs to ADMS

Heat flux: $F_{\theta 0}$ estimated from flux profile method
 LMO: L_{MO} from the flux profile method used to estimate $F_{\theta 0}$ from ADMS pre-processor
 Solar rad: Solar radiation Sellafield site measurements input to ADMS pre-processor
 NWP A & B: NWP data (cloud cover) from two closest grid points to Sellafield site input to pre-processor
 Ringway: Ringway, 2000 (cloud cover) input to ADMS pre-processor.

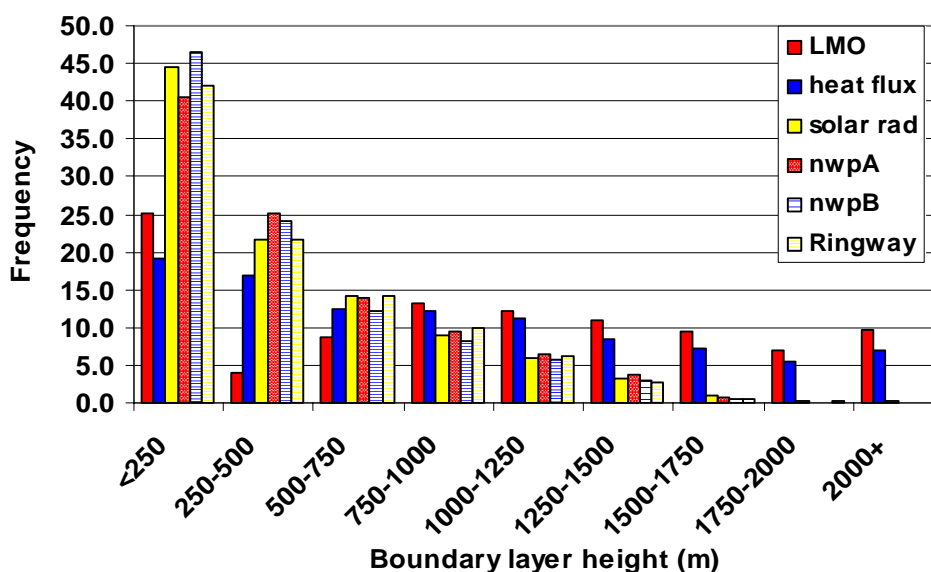


Figure 4: Binned frequency of boundary layer estimates from 5 different met data inputs to ADMS

Heat flux: $F_{\theta 0}$ from the flux profile method used to obtain h from the ADMS pre-processor
 LMO: L_{MO} from the flux profile method used to obtain h from the ADMS pre-processor
 Solar rad: Solar radiation Sellafield site measurements input to ADMS pre-processor
 NWP A & B: NWP data (cloud cover) from two closest grid points to Sellafield site input to pre-processor
 Ringway: Ringway, 2000 (cloud cover) input to ADMS pre-processor.

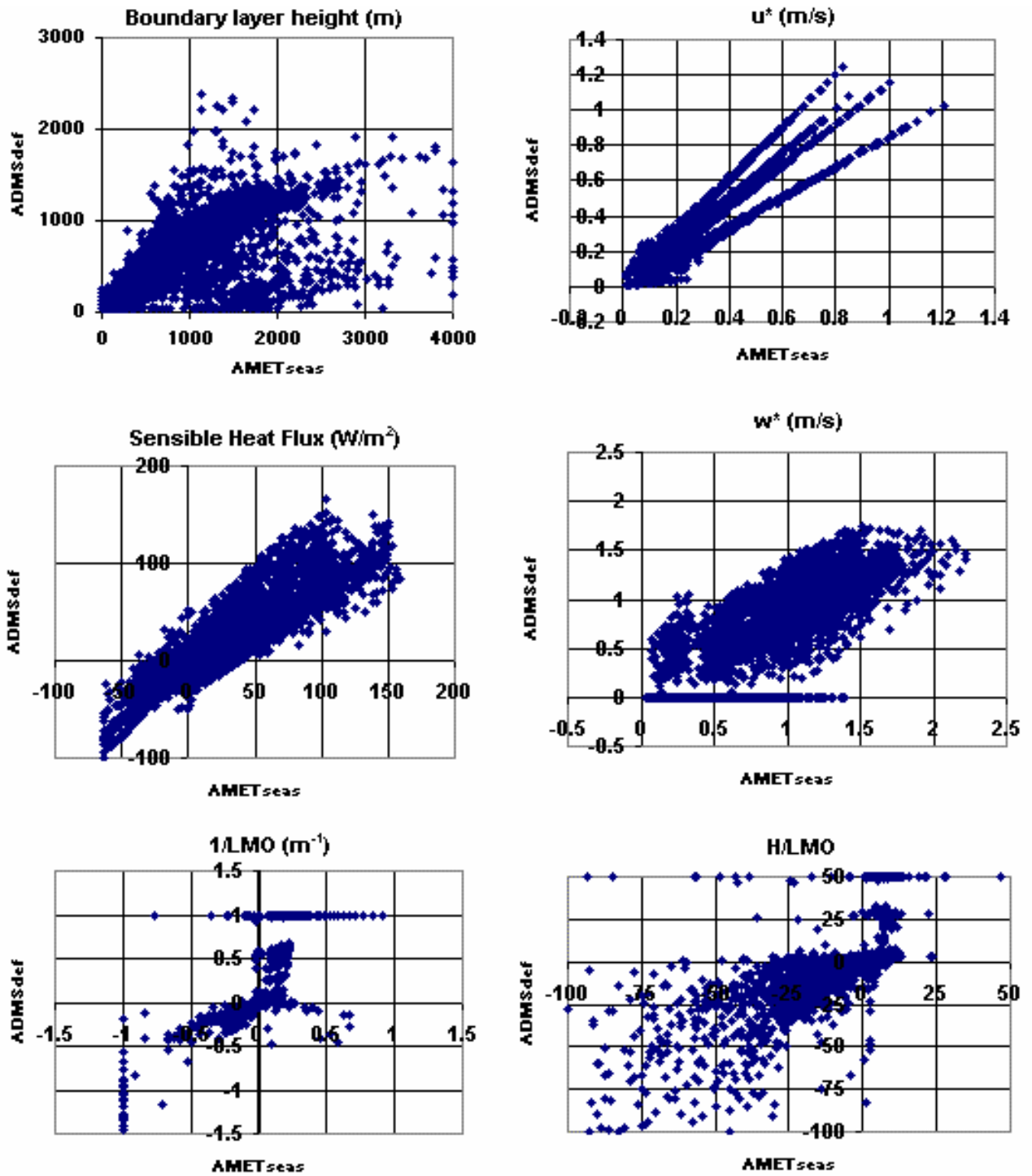


Figure 5: Correlation of boundary layer parameters between ADMS and AERMET pre-processors for Ringway, 2000

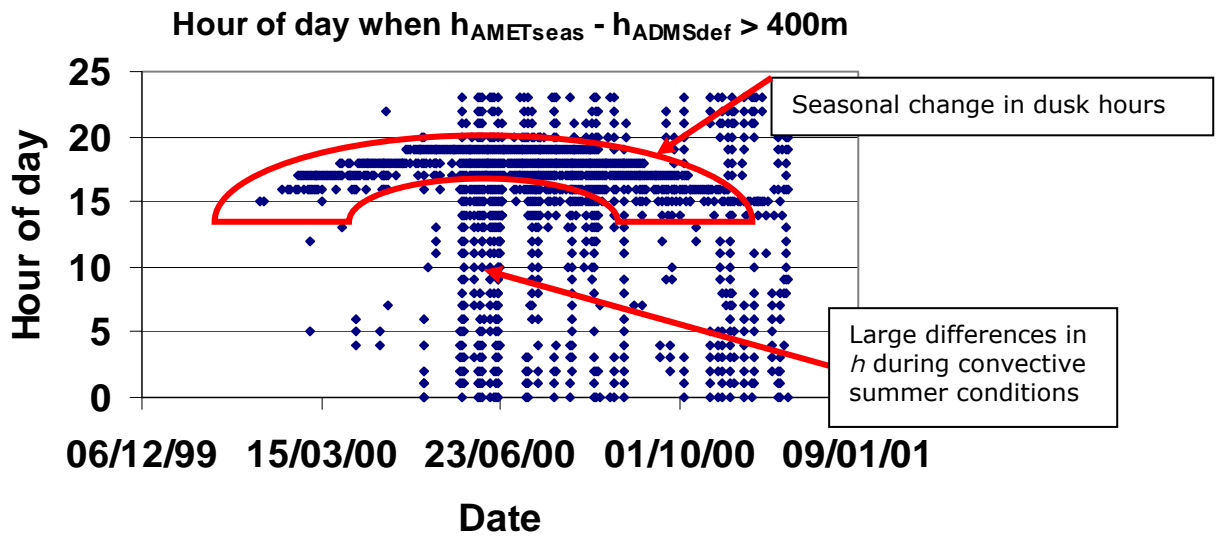


Figure 6: Hours during which disparity between ADMS and AERMET boundary layer heights are greatest

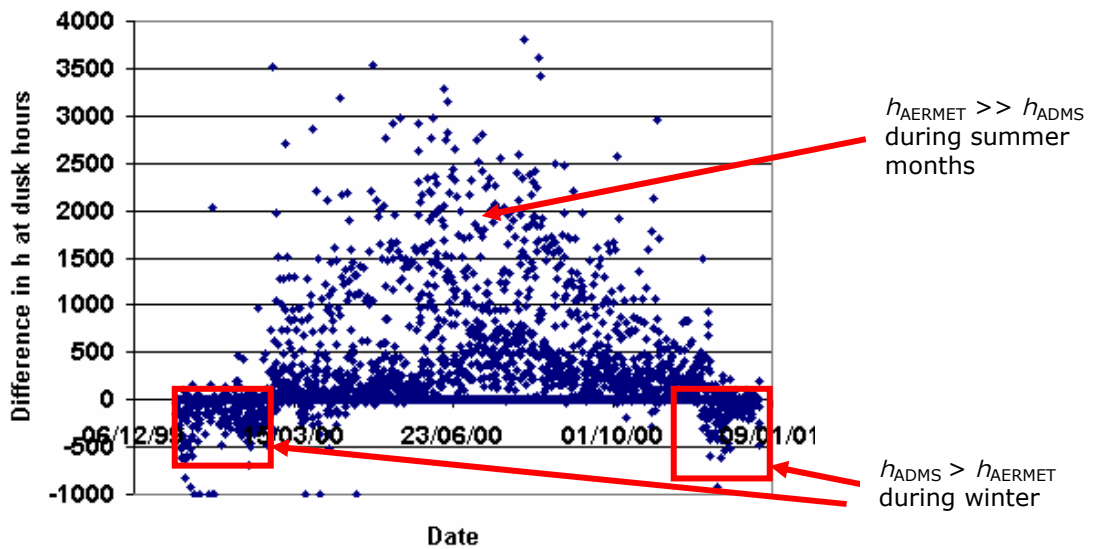


Figure 7: Seasonal dependence of boundary layer height differences between ADMS and AERMET

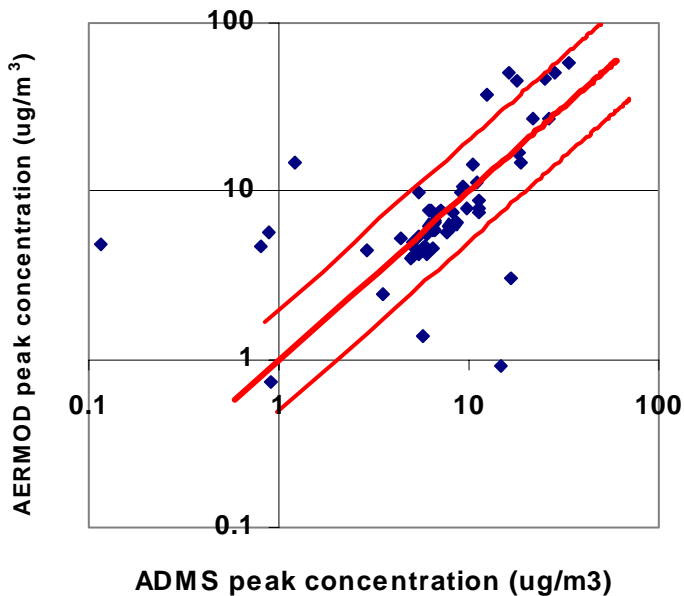


Figure 8: Correlation of peak concentrations from ADMS and AERMOD

Thick solid line indicates 1:1 agreement
 Solid lines indicate within a 2:1 agreement

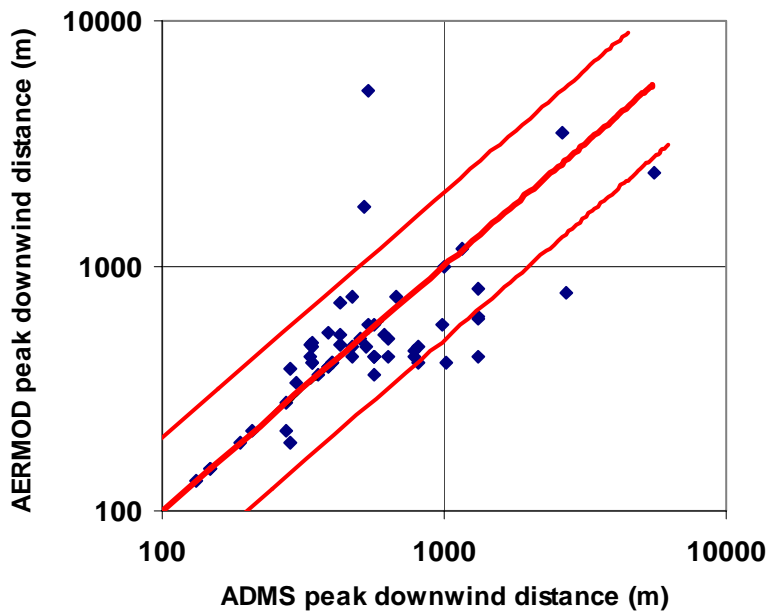


Figure 9: Correlation of downwind distance of peak concentration from ADMS and AERMOD

Thick solid line indicates 1:1 agreement
 Solid lines indicate within a 2:1 agreement

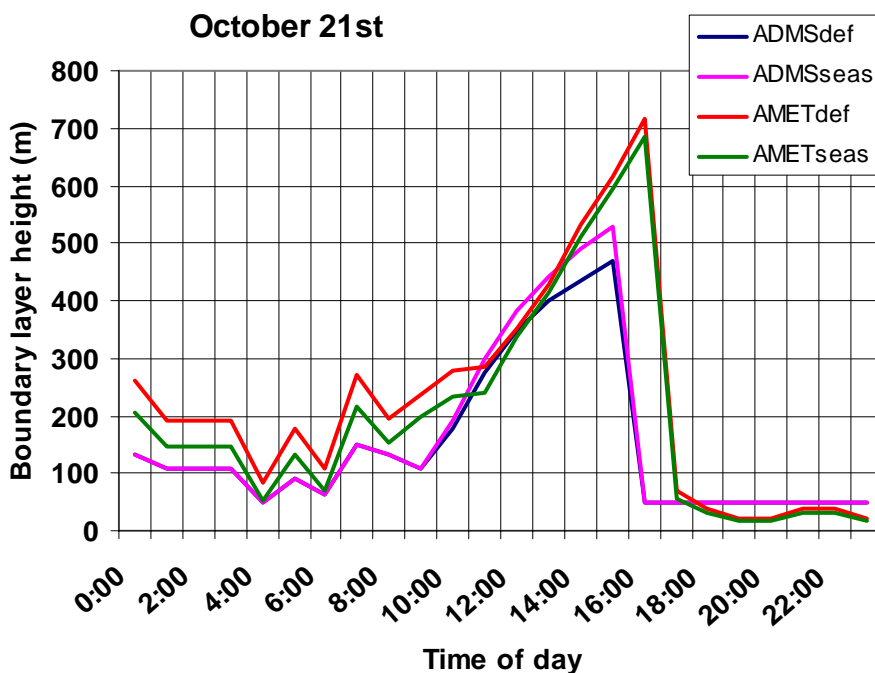


Figure 10: Boundary layer height estimates of ADMS and AERMET pre-processors for October 21st

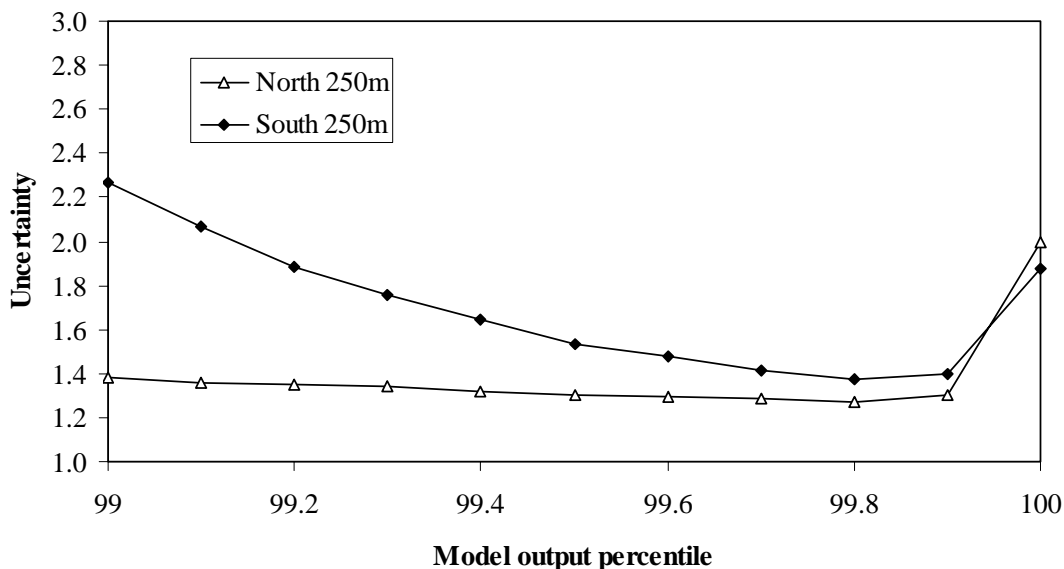


Figure 11: The relationship between uncertainty (as defined by the ratio of the 97.5th to 2.5th percentiles of the Monte Carlo simulations) and the various percentiles of the hourly concentration distribution output by ADMS

Data correspond to scenario (iii) of the Monte Carlo model and relate to a stack height of 40 m.

APPENDIX A RECONSTRUCTING TEMPERATURE AND WIND SPEED PROFILES

A1 Interpreting profiles to estimate boundary layer parameters

In Section 5.2 of this report a Monte Carlo method was presented for assessing the uncertainty in the predictions of the flux gradient micrometeorological method that arise from uncertainty in wind speed and potential temperatures. To recap, Equations A1 and A2 can be used to interpret vertical gradients in wind speed (u) and potential temperature (θ) to determine friction velocities (u_*) and eddy temperatures (θ_*). Where measurements are made at multiple heights gradients are determined from the measurement data using linear regression analysis.

$$u_* = k \frac{\partial u \{z-d\}}{\partial [\ln(z-d) + \Psi_M]} \quad \text{Equation A1}$$

$$\theta_* = k \frac{\partial \theta \{z-d\}}{\partial [\ln(z-d) + \Psi_H]} \quad \text{Equation A2}$$

Following the determination of u_* and θ_* it is relatively straightforward to calculate sensible heat flux and Monin Obukhov length for input into an atmospheric dispersion model using Equations A3 and A4.

$$F_{\theta 0} = -\rho_a C_p u_* \theta_* \quad \text{Equation A3}$$

$$L_{MO} = -\frac{\rho_a C_p (\theta + 273) u_*^3}{k g F_{\theta 0}} \quad \text{Equation A4}$$

It should however be noted that Ψ_H and Ψ_M in Equations A1 and A2 are semi-empirical stability correction terms (integrated with respect to height). We have used the derivations for a stable atmosphere of Thom (1975) (Equation A5).

$$\Psi_M = \Psi_H = \frac{5.2 (z-d)}{L_{MO}} \quad \text{Equation A5}$$

Whilst for an unstable atmosphere we have used the derivation of Paulson (1970), Equations A6, A7 and A8.

$$\Psi_M = -2\ln\left(\frac{1+x}{2}\right) + \ln\left(\frac{1+x^2}{2}\right) - 2 \text{TAN}^{-1}(x) + \frac{\pi}{2} \quad \text{Equation A6}$$

$$\Psi_H = -2\ln\left(\frac{1+x^2}{2}\right) \quad \text{Equation A7}$$

Where TAN^{-1} is in radians and

$$x = \left[1 - \frac{16(z-d)}{L_{MO}}\right]^{0.25} \quad \text{Equation A8}$$

It should be noted that Ψ_H and Ψ_M are both functions of the Monin-Obukhov length, which causes a degree of circularity in the use of this method for deriving heat fluxes and friction velocities. Consequently, these equations are often solved iteratively. An alternative to the iterative solution method was used herein. This method used the relationships between the Richardson's number (Ri) and the Monin-Obukhov length derived by Webb (1970) for stable conditions (Equation A9) and by Dyer and Hicks (1970) (Equation A10) for unstable conditions.

$$L_{MO} = \frac{[1 - (5.2Ri)](z-d)}{Ri} \quad \text{Equation A9}$$

$$L_{MO} = \frac{z-d}{Ri} \quad \text{Equation A10}$$

The Richardson's number (Ri) can be directly derived from the wind speed and temperature gradients using Equation A11 (Sutton, 1990).

$$Ri = \frac{(z-d)g \delta\theta / \delta \ln(z-d)}{\theta [\delta u / \delta \ln(z-d)]^2} \quad \text{Equation A11}$$

A2 Interpreting boundary layer parameters to estimate profiles

The previous section showed that it is relatively straightforward to determine boundary layer parameters from measurements of wind speed and temperature at a number of heights. We could therefore have used "real" field data within the Monte Carlo model detailed in Section 5.2, and applied error terms to those data and propagated the errors through Equations A1 – A11 in order to establish the uncertainty in the calculations of u^* , $F_{\theta 0}$ and L_{MO} . However an alternative method

was required, in order to relate the uncertainty in the application of the flux gradient method back to the meteorological conditions observed in the Ringway (2000) dataset.

Table 2 details the results of banding the Ringway (2000) dataset into seven discrete stability categories (A-G). This analysis provided a means of determining typical boundary layer parameters for each stability class. We then applied the flux gradient method in reverse to reconstruct the wind speed and temperature measurements that would be related to these profiles using Equations A12 and A13. The stability correction terms Ψ_H and Ψ_M were determined from the Monin Obukhov lengths using Equations A5 – A8.

$$u\{z-d\} = \frac{u_*}{k} [\ln(z-d) + \Psi_M] - \frac{u_*}{k} \ln(z_0) \quad \text{Equation A12}$$

$$\theta\{z-d\} = \frac{\theta_*}{k} [\ln(z-d) + \Psi_H] - \frac{\theta_*}{k} \ln(z\{\theta=0\}) \quad \text{Equation A13}$$

It should be noted that z_0 in Equation A12 is the roughness height and $z\{\theta=0\}$ in Equation A13 is the height at which potential temperature = 0. The value of $z\{\theta=0\}$ was determined by fitting the profile to a potential temperature, at a height of 2 m, of 15°C.

As a test of internal consistency in the above calculations, values of u_* and $F_{\theta 0}$ that were used to derive temperature and wind speed profiles (using Equations A12 and A13) were compared with those values output when the profiles were interpreted (using Equations A1-A11). For all stability classes, except G, the comparison showed the calculations were accurate to within approximately +/- 1%. A much larger calculation error was found when applying this method in category G. This was due to the very low values of both u_* and $F_{\theta 0}$, which increased the sensitivity of the method to the stability correction terms and to the assumption in Equation A11 that wind speed and temperature gradients were logarithmic.